

A Statistical Difference Reduction Method for Escaping Backdoor Detection

Pengfei Xia, Hongjing Niu, Ziqiang Li, and Bin Li, *Member, IEEE*

Abstract—While Deep Neural Networks (DNNs) deliver superior performance in many tasks, it comes at the cost of massive training resources. To save the cost, collecting data from the Internet and hiring a third party to train a model become common practices. Unfortunately, recent studies show that these operations provide a path for injecting a concealed backdoor into a DNN. An infected model behaves normally on benign inputs, whereas its prediction will be forced to an attack-specific target on adversarial data. Several detection methods have been developed to distinguish inputs to defend against such attacks. The common hypothesis that these defenses rely on is that there are large statistical differences between the latent representations of clean and adversarial inputs extracted by the infected model. However, although it is important, comprehensive research on whether the hypothesis must be true is lacking.

In this paper, we focus on it and study the following relevant questions: 1) What are the properties of the statistical differences? 2) How to effectively reduce them without harming the attack intensity? 3) What impact does this reduction have on difference-based defenses? Our work is carried out on the three questions. First, by introducing the Maximum Mean Discrepancy (MMD) as the metric, we identify that the statistical differences of multi-level representations are all large, not just the highest level. Then, we propose a Statistical Difference Reduction Method (SDRM) by adding a multi-level MMD constraint to the loss function during training a backdoor model to effectively reduce the differences. Last, three typical difference-based detection methods are examined. The F1 scores of these defenses drop from 90%-100% on the regularly trained backdoor models to 60%-70% on the models trained with SDRM on all two datasets, four model architectures, and four attack methods. The results indicate that the proposed method can be used to enhance existing attacks to escape backdoor detection algorithms.

Index Terms—Deep Neural Networks, Backdoor Attacks, Backdoor Detection, Statistical Differences, Maximum Mean Discrepancy.

1 INTRODUCTION

IN the past few years, Deep Neural Networks (DNNs) have achieved remarkable results in computer vision [1], [2], [3], [4], [5], natural language processing [6], [7], [8], and many other fields [9], [10], [11], [12]. The success of DNNs is inseparable from a large amount of training data, large-scale parameters, and powerful computing resources. For example, GPT-3 [13], a deep model that has been demonstrated to be quite effective in various language tasks, comprises 175 billion parameters and is pre-trained on about 45TB of text data. It would cost 4.6 million dollars and take 355 years to run a single training cycle of the model on a Tesla V100 GPU¹. The excellent performance of DNNs usually comes at the cost of massive time and economic resources.

To save the training cost, collecting data from the Internet, using pre-trained parameters, and commissioning a third party to train a model have become common practices for users and companies. Unfortunately, because of possible malicious sources and parties, these operations bring security risks. One of the major threats is dubbed as *backdoor attacks* or *Trojan attacks* [16], [17], [18], [19], where a hidden backdoor is injected into a victim model during the training

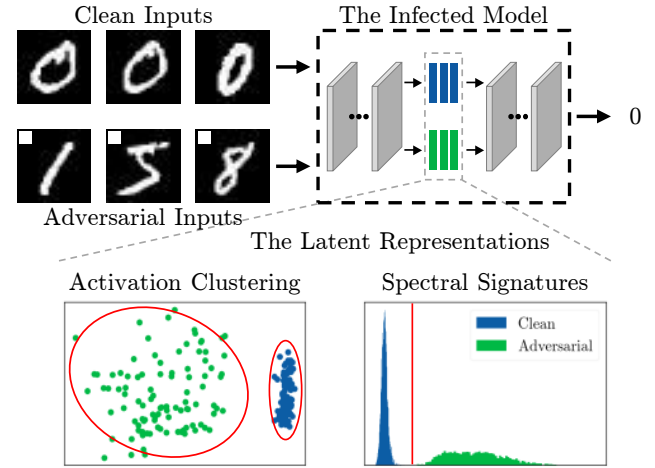


Fig. 1: An illustrating example of difference-based detection methods. The infected model is trained to classify all inputs with the trigger, i.e., a white square in the upper left corner of the images, as the number 0. Some detection defenses, such as the activation clustering [14] and the spectral signatures [15], use the hidden activations of the infected model as the latent representations of inputs to distinguish data.

• P. Xia, Z. Li and B. Li are with the Department of Electronic Engineering and Information Science, University of Science and Technology of China, Hefei, China.
E-mail: {xpengfei, iceli}@mail.ustc.edu.cn, binli@ustc.edu.cn.

• H. Niu is with the Department of Automation, University of Science and Technology of China, Hefei, China.
E-mail: sasori@mail.ustc.edu.cn.

1. <https://lambdalabs.com/blog/demystifying-gpt-3/>

stage and can be activated by a pre-defined trigger. The infected model presents two sides. On the one hand, it behaves normally like a benign one when the backdoor is not activated. On the other hand, once triggered, the output of the model will be forced to an attack-specific target. Backdoor attacks have seriously threatened the realistic

deployment of DNNs in security-sensitive scenarios, such as face recognition systems [16], [20] and autonomous cars [17].

Therefore, how to defend against such attacks is important. A vast number of detection methods [14], [15], [21], [22] address this problem by distinguishing adversarial inputs from clean benign ones. More concretely, for all instances classified into the same category by the infected model, the defenses first extract the latent representations of these inputs and then use them to separate data. For example, Chen et al. [14] proposed the activation clustering, which is based on the observation that the projected activations of the last hidden layer break out into two distinct clusters. Tran et al. [15] proposed to calculate an outlier score for each input by performing the singular value decomposition on the representations and removing inputs with the top scores. An illustrating example is shown in Figure 1.

It can be seen that the above detection methods all rely on a common hypothesis: the latent representations of clean and adversarial inputs, which are extracted by the infected model, belong to two dissimilar distributions. For convenience, we call the degree of this dissimilarity a statistical difference. One might wonder whether the hypothesis must be true. Although it is crucial for studying the effective scope of many previous defenses, few works have paid attention to it. To the best of our knowledge, there is only one most relevant study, from Tan and Shokri [23]. They used a generative adversarial network to increase the indistinguishability of the activations of the last convolutional layer between poisoned and clean inputs to bypass backdoor detection algorithms. However, due to lack of the exploration of the properties of the statistical differences, models trained with their reduction method can still be used to distinguish adversarial data, as long as the detection algorithm is slightly modified. We will discuss it in Section 5 and Section 6.

In this paper, we conduct a comprehensive study on the above hypothesis and mainly focus on the following questions:

- What are the properties of the statistical differences?
- How to effectively reduce them without harming the attack intensity?
- What impact does this reduction have on difference-based defenses?

Our work is carried out on the above three questions, and the main contributions of this paper include:

- We introduce a kernel-based metric, the Maximum Mean Discrepancy (MMD), to explicitly quantify the statistical differences between clean and adversarial inputs in the latent space and identify several properties. The most important one is that the differences of multi-level representations are all large. It inspires us to consider the multi-level features instead of just the outputs of the last hidden layer when designing a reduction method.
- A Statistical Difference Reduction Method (SDRM) is proposed by adding a multi-level MMD constraint to the loss function during training a backdoor model. The experimental results indicate that, within a certain range, the differences can be comprehensively

reduced by the method without compromising the attack power.

- We test the effects of several difference-based detection methods on the infected models trained with SDRM, and show that the performance of these defenses is significantly degraded compared to on the regularly trained backdoor models. It indicates that the proposed method can enhance existing attack methods to escape backdoor detection algorithms.

The rest of this paper is organized as follows. In Section 2, we briefly introduce the background necessary to this paper. Section 3 gives the experimental setup used in the next three sections. Section 4, Section 5, and Section 6 are our research about the three questions, respectively. Some open issues are discussed in Section 7. Related works are reviewed in Section 8. This paper is concluded in Section 9.

2 BACKGROUND

2.1 Deep Neural Networks

A deep neural network is composed of multiple layers and can be defined as $f_\theta = f_1 \circ f_2 \circ \dots \circ f_m$, where θ denotes the parameters of the model, f_1, f_2, \dots, f_{m-1} denote the $m-1$ hidden layers, and f_m denotes the output layer. For convenience, let $z_i = f_1 \circ f_2 \circ \dots \circ f_i$ denotes the structure from the input layer to the i -th hidden layer and $z_i(x)$ denotes the extracted representation of the input x . Given a training set $D = \{(x, y)\}$, the procedure of training a DNN for a classification task can be formulated as

$$\theta^* = \operatorname{argmin}_{\theta} \frac{1}{|D|} \sum_{(x,y) \in D} L(f_\theta(x), y), \quad (1)$$

where (x, y) denote the input data and its ground-truth label, and L denotes a loss function. The trained model is expected to perform well on a test set T and $D \cap T = \emptyset$ is required.

2.2 Backdoor Adversary

We consider injecting a hidden backdoor into a DNN through data poisoning [16], [17], [18], [24], [25]. Similar to the regular classification task, let U and V denote the poisoned training and test sets, respectively. The generation of poisoned data is associated with a target class t , a backdoor trigger b , and a fusion function G . For a clean sample pair (x, y) , the corresponding adversarial pair is (x', t) , where $x' = G(x, b)$ and $t \neq y$. To train a DNN with a backdoor, one can optimize

$$\theta^* = \operatorname{argmin}_{\theta} \left[\frac{1}{|D|} \sum_{(x,y) \in D} L(f_\theta(x), y) + \frac{1}{|U|} \sum_{(x',t) \in U} L(f_\theta(x'), t) \right]', \quad (2)$$

and suppose the trained model can generalize to the test sets T and V . In data poisoning, the ratio of poisoned samples to clean samples in training data, i.e., $r = |U|/|D|$, is an important hyper-parameter.

2.3 Statistical Differences

Given an infected DNN f_θ , let $Z_{ij}^T = \{z_i(x) | (x, y) \in T \wedge f_\theta(x) == j\}$ and $Z_{ij}^V = \{z_i(x') | (x', t) \in V \wedge f_\theta(x') == j\}$ denote the extracted features of clean and adversarial inputs, which are classified into the same category j by the infected model, respectively. A statistical difference refers to the degree of the dissimilarity between the distributions of Z_{ij}^T and Z_{ij}^V . In particular, since a well-trained infected model classifies almost all adversarial inputs into the target category t , we mainly focus on the difference between Z_{it}^T and Z_{it}^V . Some previous detection methods [14], [15], [21], [22] assume that the differences are large enough to distinguish poisoned data.

2.4 Maximum Mean Discrepancy

Gretton et al. [26] introduced a kernel-based metric to quantify the distance between two statistical objects. Formally, let $X_1 \sim p$ and $X_2 \sim q$ denote two sample sets drawn from the distributions p and q , respectively. In practice, MMD can be formalized as

$$\begin{aligned} MMD^2(X_1, X_2) = & \frac{1}{|X_1|(|X_1| - 1)} \sum_{x_1 \in X_1} \sum_{x'_1 \in X_1} k(x_1, x'_1) + \\ & \frac{1}{|X_2|(|X_2| - 1)} \sum_{x_2 \in X_2} \sum_{x'_2 \in X_2} k(x_2, x'_2) - \\ & \frac{2}{|X_1||X_2|} \sum_{x_1 \in X_1} \sum_{x_2 \in X_2} k(x_1, x_2) \end{aligned} \quad (3)$$

where k is a kernel function and $k(x_1, x_2) = \langle \phi(x_1), \phi(x_2) \rangle$, ϕ denotes a feature mapping. It can be seen that this metric does not require knowing the form of distributions and can be computed on high-dimensional data.

2.5 Threat Model

Our threat model considers that a user utilizes a DNN trained in an untrusted environment, e.g., a third party, to build a system to provide an external service. This mode is very common among companies, such as car manufacturers and autonomous driving solution providers. We assume that the attacker has full control over the training data and the training procedure. The goal of the defender is to distinguish malicious instances from inputs during the service time. The defender does not know any prior knowledge about the trigger, but can access to the parameters of the trained model and keep a few clean validation data.

3 EXPERIMENTAL SETUP

3.1 Datasets

Two image datasets, CIFAR-10 [27] and CelebA [28], which are often used in the research of backdoor learning [25], [29], [30], are selected. For CelebA, following the configuration in some previous studies [25], [30], we use the three most balanced attributes, i.e., "Heavy Makeup", "Mouth Slightly Open", and "Smiling", to create eight categories for the image classification task.

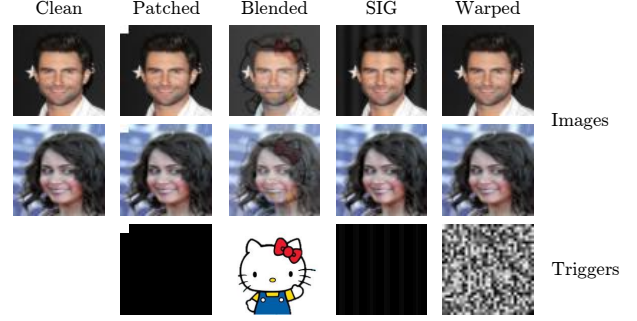


Fig. 2: Poised examples from CelebA generated by four backdoor attacks.

3.2 DNN Architectures

Four DNN architectures, VGG-11 (V-11) [31], VGG-16 (V-16) [31], ResNet-18 (R-18) [32], and PreActResNet-18 (P-18) [33], are used in our experiments. Since the activations of the hidden layer need to be extracted as the representations of inputs, we define s_1, s_2, s_3 to represent three locations in the network structure. $z_{s_1}(x), z_{s_2}(x), z_{s_3}(x)$ denote the extracted features of x from the corresponding levels. Specifically, we set s_1, s_2, s_3 to the 14th, 21st, 28th layers for V-11, the 23rd, 33rd, 43rd layers for V-16, and the 27th, 39th, 51st layers for R-18 and P-18.

3.3 Attack Methods

Four poisoning-based attack methods are considered, including the patch-based attack (Patched) [17], the blending-based attack (Blended) [16], SIG [24], and the warping-based attack (Warped) [25]. The main differences between these attacks are the trigger b and the fusion function G . The forms of generating backdoor samples are shown in Table 1 and some poisoned examples from CelebA are shown in Figure 2. Except for the different ways of constructing adversaries, we keep the other setting the same. The target t is set to the 0th category and the poisoning data ratio, r , is set to 0.1.

TABLE 1: Forms of generating backdoor samples. m : a 2D mask. α : a hyper-parameter between 0 to 1. W : the warp function.

Attack	Fusion Function $x' = G(x, b)$
Patched	$x' = (1 - m) \odot x + m \odot b$
Blended	$x' = (1 - \alpha) \cdot x + \alpha \cdot b$
SIG	$x' = x + b$
Warped	$x' = W(x, b)$

3.4 Defense Methods

Four defenses are tested in this paper, three of which are difference-based detection methods. It should be noted that some of these methods are proposed to filter data during the training phase, but we use them on test data here and find that they also have good performance. Besides, the original detection methods mainly utilize the outputs of the last hidden layer to distinguish data, we extend them to multiple levels for a more thorough analysis.

3.4.1 Activation Clustering

Chen et al. [14] proposed the activation clustering to detect poisoned data, which does not require verified and trusted data. The author first observed that the features of clean and adversarial inputs, which are classified into the same category by the poisoned model, visually show two distinct clusters. Then they proposed to filter poisoned data with three steps: 1) perform the independent component analysis on the latent representations to reduce the dimensionality, 2) use the k-means algorithm to cluster the reduced features into two clusters, and 3) analyze whether each cluster is clean or adversarial through the exclusionary reclassification, the relative size comparison, or the silhouette score.

3.4.2 Spectral Signatures

Tran et al. [15] identified a new property, called spectral signatures, of backdoor attacks. A spectral signature is a detectable trace in the spectrum of the covariance of the representations that these attacks tend to leave behind. Then, they presented an algorithm to show that one can use this trace to remove adversarial inputs: 1) perform the singular vector decomposition on the centered features, 2) calculate the outlier scores with the top right singular vector, and 3) remove data with the top-k scores.

3.4.3 Subspace Reconstruction

The core idea of the subspace reconstruction for detecting a backdoor is to construct a subspace learned from a small number of clean features, and assume that projecting adversarial features into this space will cause a lot of information to be lost. Therefore, these features have higher reconstruction losses than clean ones. Javaheripi et al. [34] first introduced this idea into their Trojan detection framework.

3.4.4 Neural Cleanse

Wang et al. [35] presented the neural cleanse, a detection and mitigation system for backdoor attacks. In the detection step, the method first uses the reverse engineering to obtain potential triggers towards every category, and then determine the final synthetic trigger according to its l_1 norm. Wang et al. [35] introduced three techniques, i.e., the input filtering, the neuron pruning, and the unlearning, in the mitigation step to remove the backdoor with the synthetic trigger. Because the input filtering is similar to the three detection methods described above, the unlearning needs to retrain the model, we apply the neuron pruning as the mitigation technique in this paper.

3.5 Evaluation Metrics

Evaluation metrics adopted in this paper are introduced here. We use the Benign Accuracy (BA) and the Attack Success Rate (ASR) to denote the performance of an infected model on the test sets T and V , respectively. For a difference-based detection method, we use the F1 score to evaluate its performance [36].

3.6 Implementation Details

For all experiments, we adopt the stochastic gradient descent with momentum of 0.9 and weight decay of 5e-4 as the optimizer. The batch size is set to 256 and the total training duration is 100 epochs for CIFAR-10 and 40 epochs for CelebA. The initial learning rate is set to 0.01 and is dropped by 10 after 50 and 70 epochs for CIFAR-10, 20 and 30 epochs for CelebA. All images are resized to 32×32 and normalized between 0 to 1. Our experiments are implemented with PyTorch [37] and run on a Tesla V100 GPU.

4 EXPLORATION OF THE PROPERTIES

What are the properties of the statistical differences? In this section, we try to answer this question. Before exploring the properties, we need to quantify the differences first. We notice that the representations are high dimensional data and their distributions are hard to solve explicitly. These reasons prompt us to choose MMD as the distance metric.

To analyze the differences comprehensively, we calculate the MMD values on the test data at multiple levels, i.e., $MMD^2(Z_{it}^T, Z_{it}^V)$, where $i = \{s_1, s_2, s_3\}$ and a Gaussian mixture kernel is adopted. To give intuitive comparisons, for each type of attack, we provide the intra-class and minimal inter-class distances between clean samples as two baselines, that is, $MMD^2(Z_{it}^T, Z_{it}^T)$ and $\min_{j \neq t} MMD^2(Z_{it}^T, Z_{ij}^T)$. For the intra-class distance, we sample two sets from Z_{it}^T to calculate the value. The quantification results are presented in Table 2.

Some properties can be identified from the above results:

- The statistical differences of multi-level features are all large. We observe that, for all types of backdoor attacks, all model architectures, and both two datasets, there are strong increases in the MMD values compared to the corresponding intra-class distances, at all three levels. The comparison with the minimal inter-class distances is more intuitive, where the values between clean and adversarial representations are greater than the inter-class ones. Both of the two observations provide strong evidence of this property.
- The statistical differences are related to the model architecture, the form of the trigger, and the dataset. Compared to V-11 and V-16, R-18 and P-18 have smaller values in almost all cases. This seems to indicate that the models using these architectures are more difficult to defend. The warping-based attack tends to leave larger traces in the feature space than the other three attacks. This inspires us to consider whether one can reduce the differences by designing the form of the trigger. We will discuss it in Section 7. Besides, in general, the infected models trained on CelebA have larger MMD values than the models trained on CIFAR-10.

To this paper, the first property is more helpful. Since the statistical differences are large at multi-levels features, does it mean that the previous detection methods can be extended to multiple levels? We conduct experiments on it and find that this is indeed the case. The results are shown in Figure 5, Figure 6, and Figure 7, where the F1 scores of

TABLE 2: MMD values between the latent representations of clean and adversarial inputs at three levels. All values are averaged over sets of 500 inputs sampled randomly from the particular data.

Dataset	Method	V-11			V-16			R-18			P-18		
		s_1	s_2	s_3									
CIFAR-10	Patched	0.408	0.846	2.875	0.574	1.768	3.163	0.287	0.601	1.878	0.284	0.377	1.174
	Intra-class	0.013	0.013	0.018	0.014	0.016	0.010	0.015	0.014	0.015	0.016	0.013	0.015
	Inter-class	0.201	0.440	2.378	0.252	0.880	3.898	0.169	0.259	1.050	0.158	0.296	2.121
	Blended	0.265	0.921	2.960	0.387	1.639	3.790	0.281	0.305	1.046	0.285	0.381	2.513
	Intra-class	0.014	0.015	0.014	0.014	0.013	0.015	0.014	0.015	0.013	0.015	0.014	0.012
	Inter-class	0.199	0.436	2.498	0.239	1.010	4.094	0.185	0.259	1.117	0.171	0.300	2.430
	SIG	0.274	0.939	3.383	0.582	1.889	3.474	0.371	0.471	1.505	0.344	0.501	2.122
	Intra-class	0.014	0.015	0.014	0.014	0.014	0.012	0.014	0.014	0.013	0.015	0.014	0.013
	Inter-class	0.184	0.440	2.631	0.248	0.958	4.060	0.200	0.267	1.181	0.187	0.289	2.502
CelebA	Warped	0.729	1.474	3.627	1.224	1.695	4.040	0.460	0.582	1.052	0.420	0.525	1.830
	Intra-class	0.015	0.016	0.010	0.015	0.013	0.010	0.015	0.014	0.014	0.014	0.014	0.012
	Inter-class	0.194	0.459	2.533	0.241	0.953	3.978	0.188	0.279	1.233	0.172	0.298	2.321
	Patched	0.605	2.349	3.152	1.287	3.656	3.262	0.277	1.214	3.604	0.282	1.517	3.330
	Intra-class	0.022	0.017	0.020	0.023	0.014	0.035	0.018	0.018	0.020	0.020	0.020	0.013
	Inter-class	0.092	0.543	1.479	0.257	1.330	1.567	0.070	0.370	1.079	0.073	0.419	1.434
	Blended	0.257	1.769	3.503	0.800	3.558	3.824	0.219	0.720	4.021	0.205	1.072	4.695
	Intra-class	0.020	0.022	0.015	0.020	0.015	0.017	0.020	0.021	0.015	0.018	0.020	0.013
	Inter-class	0.084	0.565	1.375	0.246	1.244	1.610	0.083	0.328	1.164	0.072	0.411	1.413
	SIG	0.299	2.161	3.774	1.078	3.964	3.522	0.244	1.088	4.219	0.268	1.412	4.384
	Intra-class	0.018	0.022	0.015	0.019	0.013	0.019	0.020	0.018	0.012	0.019	0.018	0.021
	Inter-class	0.093	0.536	1.491	0.234	1.239	1.677	0.076	0.379	1.162	0.074	0.450	1.482
	Warped	0.826	2.698	3.880	1.911	4.315	4.214	0.418	1.704	4.576	0.533	2.817	4.845
	Intra-class	0.020	0.020	0.013	0.020	0.019	0.021	0.021	0.018	0.025	0.019	0.020	0.015
	Inter-class	0.093	0.597	1.304	0.232	1.272	1.676	0.078	0.397	1.171	0.077	0.462	1.536

the three defenses at three levels on the regularly trained models are all high. It provides guidance for us to design the reduction method.

5 REDUCTION OF THE DIFFERENCES

In this section, we try to answer the question of how to effectively reduce the statistical differences. According to the analysis in Section 4, we can know that the differences of multi-level features are all large and can be used to distinguish adversarial data. So we propose a method, named SDRM, to reduce the differences by adding a multi-level MMD constraint to the loss during training a backdoor model. The proposed method can be formulated as:

$$\theta^* = \underset{\theta}{\operatorname{argmin}} \left[\frac{1}{|D|} \sum_{(x,y) \in D} L(f_{\theta}(x), y) + \frac{1}{|U|} \sum_{(x',t) \in U} L(f_{\theta}(x'), t) + , \frac{1}{|I|} \sum_{i \in I} MMD^2(Z_{it}^D, Z_{it}^U) \right] \quad (4)$$

where I is a set of levels, and λ is a hyper-parameter that controls the constraint strength. From the formula, the optimization goal consists of three parts, where the first two are included in the regular backdoor training, as shown in Equation 2. We add the third item in the training to achieve the purpose of reducing the statistical differences. In practice, we adopt the mini-batch training and the procedure is presented in Algorithm 1.

In the experiments, we consider two settings of I , namely $I = \{s_3\}$ and $I = \{s_1, s_2, s_3\}$, which correspond

Algorithm 1: Mini-batch SDRM

Input: Clean training set D ; Poisoned training set U ; Learning rate η ; Number of training epochs N ; Constraint strength λ ; Feature level set I ; Target label t

Output: Model parameters θ

- 1 Initialize parameters θ ;
- 2 Create the concatenated training set $C = D \cup U$;
- 3 **for** $n \leftarrow 1$ **to** N **do**
- 4 Shuffle the training set C ;
- 5 **for** each mini-batch $(X, Y) \subset C$ **do**
- 6 $(X_1, Y_1) = \{(x, y) \mid (x, y) \in (X, Y) \wedge (x, y) \in D\}$;
- 7 $(X_2, Y_2) = \{(x, y) \mid (x, y) \in (X, Y) \wedge (x, y) \in U\}$;
- 8 $(X_3, Y_3) = \{(x, y) \mid (x, y) \in (X, Y) \wedge (x, y) \in D \wedge y == t\}$;
- 9 $L_1 \leftarrow \frac{1}{|X_1|} \cdot L(f_{\theta}(X_1), Y_1)$;
- 10 $L_2 \leftarrow \frac{1}{|X_2|} \cdot L(f_{\theta}(X_2), Y_2)$;
- 11 $L_3 \leftarrow \frac{1}{|I|} \cdot \sum_{i \in I} MMD^2(Z_i^{X_2}, Z_i^{X_3})$;
- 12 $L_t \leftarrow L_1 + L_2 + \lambda \cdot L_3$;
- 13 $\theta \leftarrow \theta - \eta \cdot \nabla_{\theta} L_t$;
- 14 **end**
- 15 **end**

to constraining the features of the last hidden layer (SDRM-L) and all three levels (SDRM-A), respectively. We set $\lambda = \{0.0, 0.1, 0.2, 0.3\}$, where $\lambda = 0.0$ stands for the Regular Backdoor Training (RBT). For convenience, we use

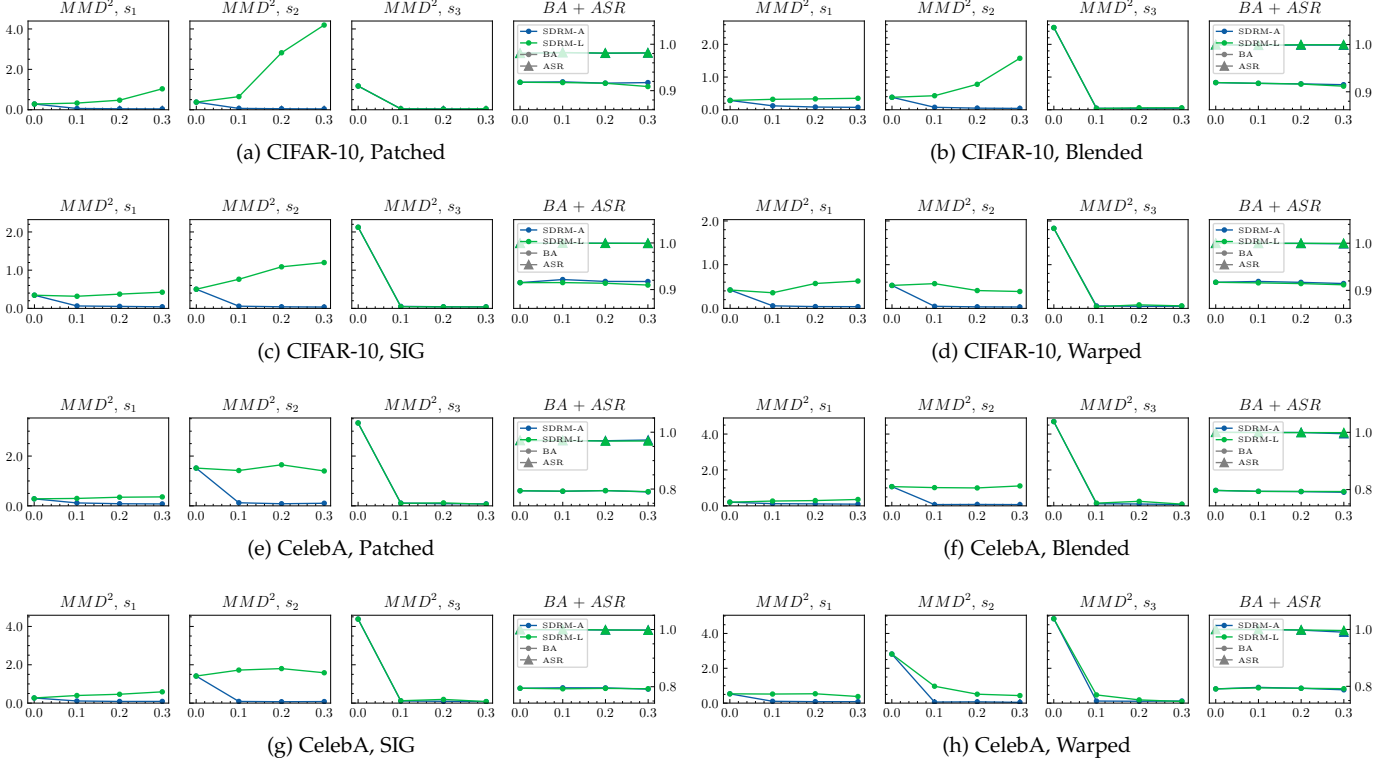


Fig. 3: Results of SDRM on the {P-18} models with different λ . X-axis: the value of λ . Y-axis: the value of each indicator.

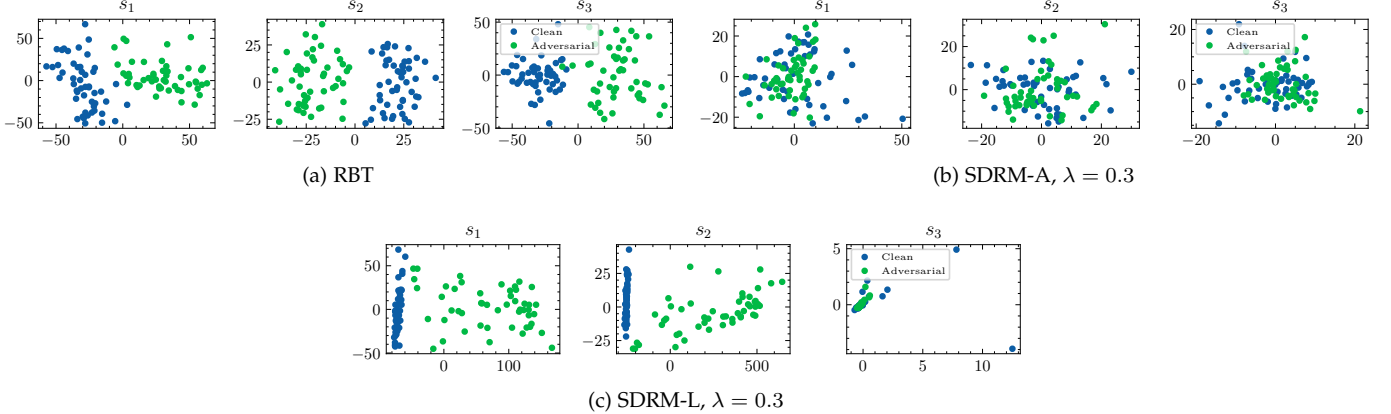


Fig. 4: Visualization examples of the features extracted from the {CIFAR-10, P-18, Patched} models. X-axis: the first dimension. Y-axis: the second dimension.

the {A,B,C} model to denote the infected model trained on dataset A with architecture B and attack method C. The experimental results on the {P-18} models are shown in Figure 3. The results on other structures are similar and are shown in Appendix.

Some observations are summarized as follows:

- The statistical differences at multi-level features can be significantly reduced by the proposed SDRM-A without harming the attack power. For example, when $\lambda = 0.3$, the poisoned models sacrifice averaged 0.15% of BA and 0.11% of ASR for averaged 84.6%, 91.2%, and 97.7% reduction of MMD^2 at s_1 ,

s_2 , and s_3 for CIFAR-10, and sacrifice averaged 0.53% of BA and 0.96% of ASR for averaged 69.6%, 94.9%, and 98.0% reduction of MMD^2 at s_1 , s_2 , and s_3 for CelebA, respectively.

- Constraining only the features of the last hidden layer, i.e., SDRM-L, causes the features of other intermediate layers to still have large differences. Also take the case of $\lambda = 0.3$ as an example, the averaged reductions at s_1 , s_2 , and s_3 for SDRM-L are -89.9%, -360.0%, and 97.1% for CIFAR-10, and -48.0%, 19.2%, and 98.1% for CelebA, respectively. It can be seen that the differences at the first two levels may be greatly increased with SDRM-L, which preserves the

possibility for using these features to defend. These results demonstrate that the method of constraining only the last layer [23], is not sufficient.

In order to show the differences more intuitively, we use the dimensionality reduction to visualize the features, as shown in Figure 4. In the model trained with RBT, the features of clean and adversarial inputs can obviously be divided into two groups. For the model trained with SDRM-A, these two types of features almost overlap at all three levels. The first two levels of features are still distinguishable for the model trained with SDRM-L. The visualization results support our observations.

6 EXPERIMENTS ON DEFENSE METHODS

Since the proposed SDRM is feasible in reducing the statistical differences effectively without harming the attack intensity, in this section, we consider what impact this reduction has on difference-based defenses. Four typical methods, including the Activation Clustering (AC) [14], the Spectral Signatures (SS) [15], the Subspace Reconstruction (SR) [34], and the Neural Cleanse (NC) [35], are selected as the test subjects. The first three ones are difference-based detection methods and the last one is not. We use the infected models trained with RBT, SDRM-A, and SDRM-L to examine these defenses, where $\lambda = 0.3$.

6.1 Results of AC, SS, and SR

AC, SS, and SR are all difference-based detection methods that distinguish adversarial data from clean ones by using the latent representations of inputs extracted by the infected model. In our experiments, these methods are performed on the three levels of representations, i.e., s_1 , s_2 , and s_3 , respectively. Because the effects of the three methods are affected by the number of samples N and the ratio of poisoned inputs to clean inputs r' , we set up four combinations for each defense. The detection performance of AC, SS, and SR is measured by the F1 score, and the results on the {P-18} models are shown in this section. The results on other architectures are similar and are presented in Appendix. Below we first show the results of each defense separately and then make a unified summary.

6.1.1 Activation Clustering

As suggested in [14], we first adopt the independent component analysis to reduce the dimensionality of the latent representations of inputs to obtain the vectors of length 20. Then we use the k-means algorithm to cluster the reduced representations into two groups. The results of AC on the {P-18} models are shown in Figure 5.

6.1.2 Spectral Signatures

Following the same steps in [15], we first take the singular value decomposition of the latent representations and then use the top right vector to compute an outlier score for each input. The results of SS on the {P-18} models are shown in Figure 6.

6.1.3 Subspace Reconstruction

We choose 1% clean data as the filtered benign samples and construct a subspace that can restore 90% of the energy of these samples. Subsequently, for the representation of each input, we perform the projection and reconstruction steps with the learned subspace and compute the l_2 norm as the reconstruction loss for that sample. By adjusting the threshold, the max F1 score for each model is calculated, and the results are shown in Figure 7.

6.1.4 Summary

The experimental results of the above three defense methods are similar and are summarized as follows:

- The representations at s_1 and s_2 levels can be used by these methods to distinguish data. For example, when $N = 100$ and $r' = 1.0$, the averaged F1 scores of AC at the three levels for RBT are 0.978, 0.991, and 0.948 on the {CIFAR-10, P-18} models, and 0.898, 0.963, and 0.939 on the {CelebA, P-18} models. It confirms the conclusion in Section 4.
- The performance of difference-based detection methods is com dropped on the infected models trained with SDRM-A. For example, when $N = 500$ and $r' = 1.0$, the averaged F1 values of AC at the three levels for SDRM-A drop from 0.986, 0.997, 0.979 to 0.598, 0.546, 0.645 on the {CIFAR-10, P-18} models, and from 0.965, 0.975, 0.988 to 0.630, 0.618, 0.613 on the {CelebA, P-18} models. The results of SS and SR are similar.
- The models trained with SDRM-L can still be utilized by these defenses to detect adversarial data. For example, when $N = 500$ and $r' = 1.0$, the averaged F1 scores of AC, SS, and SR at s_0 level for SDRM-L are 0.962, 0.985, 0.867 on the {CIFAR-10, P-18} models, and 0.977, 0.998, 0.856 on the {CelebA, P-18} models. Sometimes, the values are higher than on the models trained with RBT. It indicates that only constraining the activations of the last hidden layer, which is adopted by the previous method [23], is not enough for bypassing backdoor detection algorithms.

6.2 Results of NC

NC consists of two steps, i.e., the trigger synthesis and the neuron pruning, to complete the detection and mitigation of the backdoor. We conduct experiments on the above two steps separately.

6.2.1 Trigger Synthesis

Wang et al. [35] defined a generic form of backdoor sample generation with a 3D trigger pattern and a 2D location mask. Then they formulated an optimization problem to reverse a pattern and a location for each category. The final synthetic trigger is selected by calculating the l_1 norm of all candidate masks. Because the form defined above is mainly used to reverse the patching-based attack [17], we carry out experiments on the {Patched} models. The results are shown in Figure 8 and some reversed triggers on the {CIFAR-10, Patched} models are shown in Figure 9.

As we can see, whether it is from the distinguishability of the l_1 norm or the intuitive feeling, the infected models

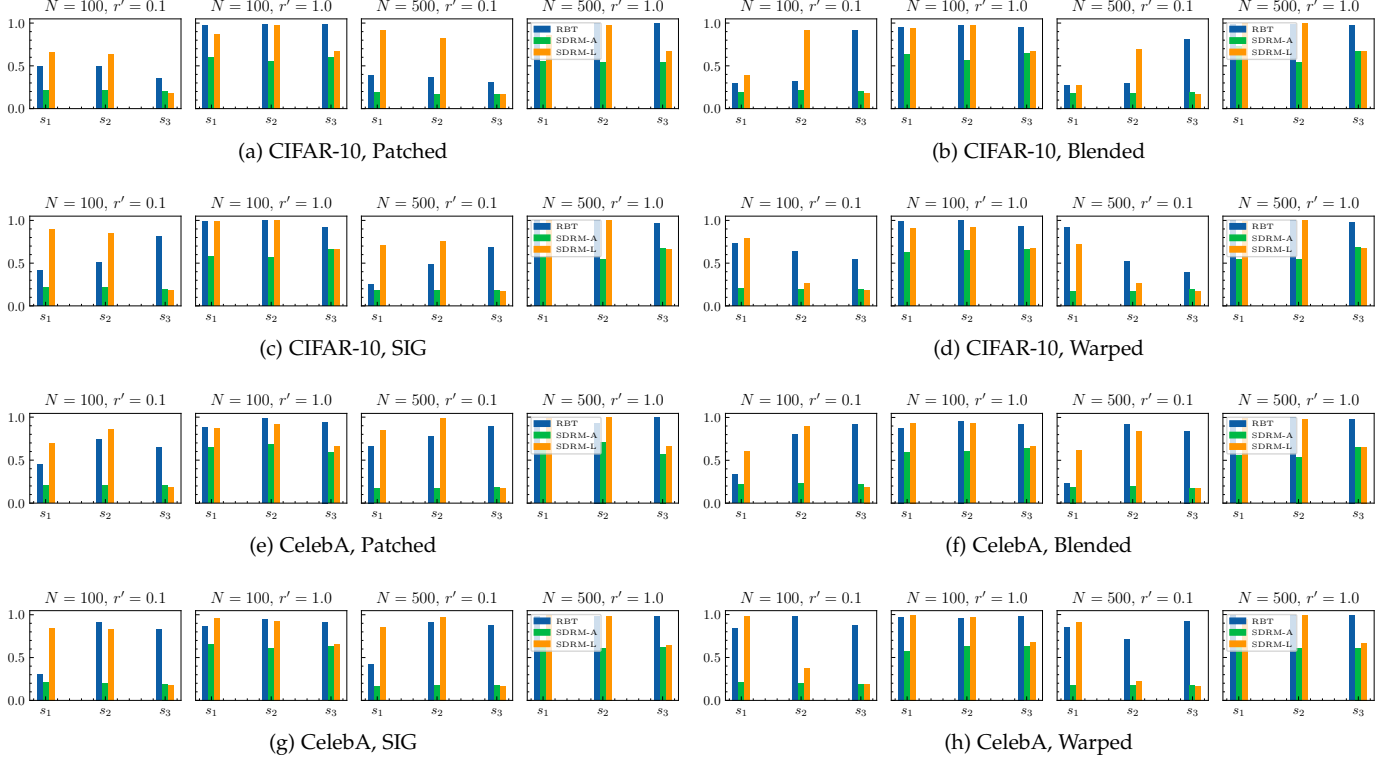


Fig. 5: F1 score of AC on the {P-18} models. X-axis: the level of features. Y-axis: the value of $F1$.

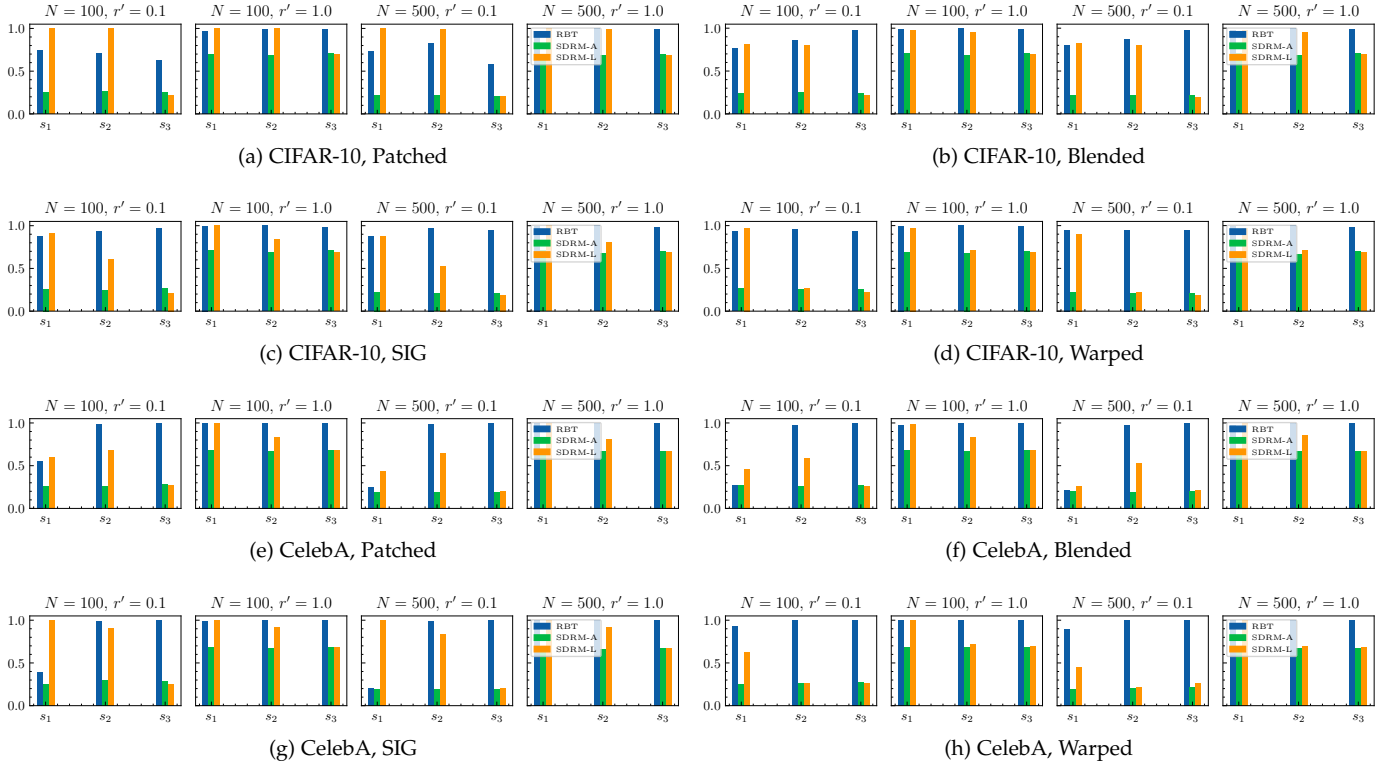


Fig. 6: F1 score of SS on the {P-18} models. X-axis: the level of features. Y-axis: the value of $F1$.

trained with SDRM can still be used to reverse the triggers. It indicates that the trigger synthesis relies on a different principle from difference-based methods to defend against

backdoor attacks. However, this method seems to be easily affected by the dataset, such as the performance on the {CelebA, Patched} models is not as good as on the {CIFAR-

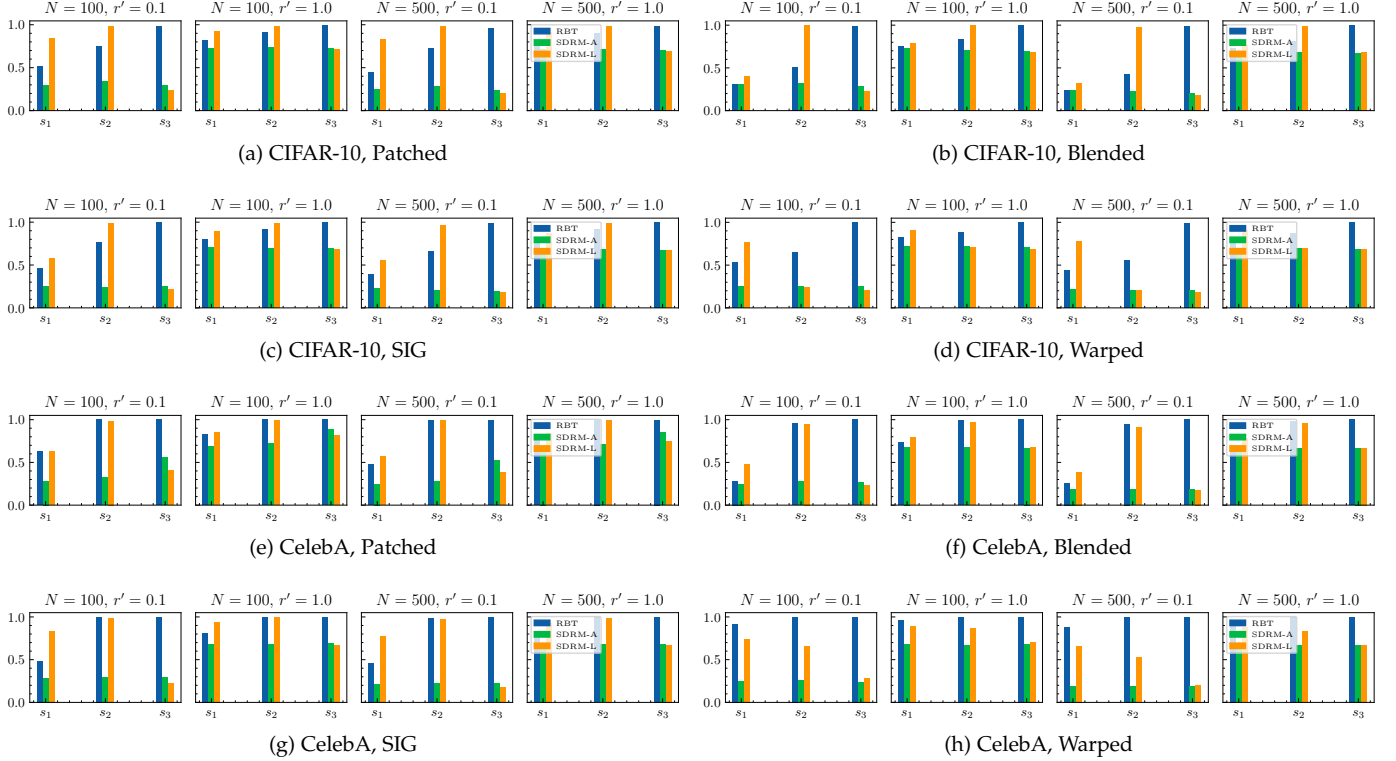


Fig. 7: F1 score of SR on the {P-18} models. X-axis: the level of features. Y-axis: the value of $F1$.

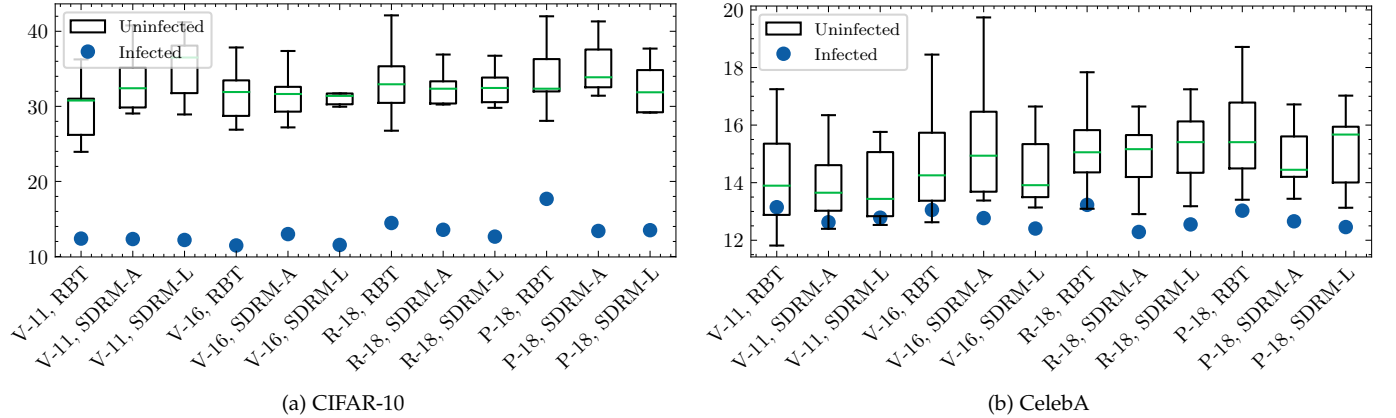


Fig. 8: l_1 norm of triggers for infected and uninfected labels on the {Patched} models. X-axis: the model architecture and the backdoor training method. Y-axis: the l_1 norm of trigger.

10, Patched} models.

6.2.2 Neuron Pruning

After obtaining the reversed trigger, Wang et al. [35] used it to patch the infected model by the neuron pruning. In our experiments, to rigorously test the proposed method, we use the real trigger instead of the reversed one for pruning. The results are shown in Figure 10.

It can be seen that the the curves of BA and ASR are affected by SDRM-A. For example, on the {CIFAR-10, V-11, Warped} models, the two curves almost overlap, showing similar downward trends. On the {CelebA} models, in most cases, BA and ASR quickly drop to low values simultane-

ously. The results indicate that the performance of the neuron pruning is reduced on the models trained with SDRM-A compared to on the models trained with RBT. We think these results are reasonable, because the neuron pruning essentially assumes that the backdoor behavior is encoded into some neurons, which is similar to the hypothesis of the statistical differences.

6.3 Kernels

Considering that the choice of a kernel in MMD may have an impact on the training of the backdoor model, we conduct experiments on different kernels, including the Gaussian Kernel (GK), the Gaussian Mixture Kernel (GMK),

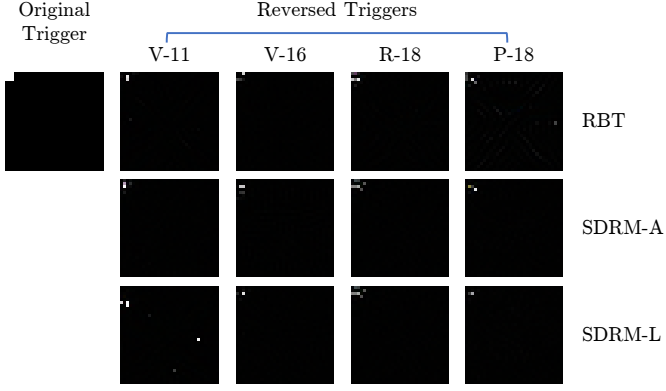


Fig. 9: Reversed triggers on the {CIFAR-10, Patched} models.

and the Linear Kernel (LK). The detailed settings are shown in Table 3. The results of three difference-based defenses are shown in Figure 11.

TABLE 3: Settings of different kernels. σ : the standard deviation.

Kernel	Parameter
GK1	$\sigma = 1/2$
GK2	$\sigma = 1$
GK3	$\sigma = 2$
GMK1	$\sigma = [1/2, 1, 2]$
GMK2	$\sigma = [1/4, 1/2, 1, 2, 4]$
GMK3	$\sigma = [1/8, 1/4, 1/2, 1, 2, 4, 8]$
GMK4	$\sigma = [1/3, 1, 3]$
GMK5	$\sigma = [1/9, 1/3, 1, 3, 9]$
GMK6	$\sigma = [1/27, 1/9, 1/3, 1, 3, 9, 27]$
LK	-

Three observations can be seen from the figure. First of all, no matter which kernel is used, SDRM significantly reduces the detection effects. Second, GK or GMK is a better choice than LK. We believe that the reason is that these two types of kernels map the original dimensions to infinite dimensions, which makes the measurement of MMD more accurate. Last, for GK and GMK, hyper-parameters have little effect on the results.

7 DISCUSSION

One of the trends in backdoor attacks is to be more concealed, where this concealment is reflected in two aspects. On the one hand, the attacker hopes that the constructed trigger can evade human perception, so some researchers have proposed the invisible attacks [38], [39] and the label-consistent attack [29]. On the other hand, the attack method needs to be machine imperceptible, that is, to escape various backdoor defenses. Some methods have been proposed to achieve the goal, including new trigger forms [25] or backdoor training approaches [23]. Our work also belongs to one of these. However, it is not sufficient to consider machine perception or human perception alone, because the defender may set up multiple defense methods. How to construct an attack that can bypass defenses with different principles requires further research.

The proposed method in this paper is to reduce the statistical differences by adding a constraint to the loss function during training a backdoor model. It requires the attacker to have permission to train the model. Another more relaxed setting is that the attacker only provides data, and the user trains the model on the data. So can the statistical differences still be reduced in this case? Based on two reasons, we argue the answer is positive. First, our work demonstrates that it is achievable to greatly reduce the differences without affecting the strong attack. Second, the experimental results in Section 6 indicate that the differences are affected by the form of trigger. However, by trying to combine the optimized triggers [40] and MMD, we make a preliminary attempt and find it is not easy. We optimize a trigger on a trained benign model, so that adding the trigger to a clean sample can not only force the model’s output into a specified category, but also minimize the statistical differences of the latent representation. Subsequently, we use this optimized trigger to construct a poisoning training set, and train an infected model on these data with RBT. The new model can always optimize parameters that are easier to complete the task but are less concealed. We plan it in future work.

8 RELATED WORK

8.1 Backdoor Attacks

Since Gu et al. [17] first explored the backdoor vulnerability in deep learning models, many variants have been proposed. From the way of injecting the hidden threat, backdoor attacks can be roughly divided into two categories, i.e., poisoning-based attacks and non-poisoning-based attacks. Poisoning-based methods [16], [17], [18], [25], [29], [39], [41] execute the Trojan horse implantation by mixing a small number of malicious samples into the training data and learning an infected model from the mixed dataset. How to construct more concealed and effective poisoned samples is the research focus of this type of attack. The primary method [17] uses a static local patch as the trigger. To obtain better attack performance, Liu et al. [18] built a Trojan method, in which the trigger is optimized rather than pre-defined. Liao et al. [38] argued that the triggers of the previous attacks [17], [18] are all visually visible, which undermines the concealment of the backdoor. Then they proposed to add an imperceptible perturbation mask to the clean image to generate its backdoor adversary. However, these attacks ignore that the inconsistency of the instance and its label can increase the risk of disclosure. Turner et al. [29] first pointed out this problem and proposed the label-consistent backdoor attacks by leveraging adversarial examples and generative models. In addition to the above-mentioned digital attacks, some studies focus on the physical world. Chen et al. [16] adopted a pair of glasses as the physical trigger to fool a face recognition system. Li et al. [42] suggested that physical transformations should be considered when training a backdoor model.

Non-poisoning-based methods [43], [44], [45], [46], [47] encode the backdoor functionality into deep models by transfer learning or weight perturbations. Dumford and Scheirer [43] first explored the possibility of injecting the backdoor without poisoning, where they proposed to modify the model’s parameters directly. Different from [43], Tang

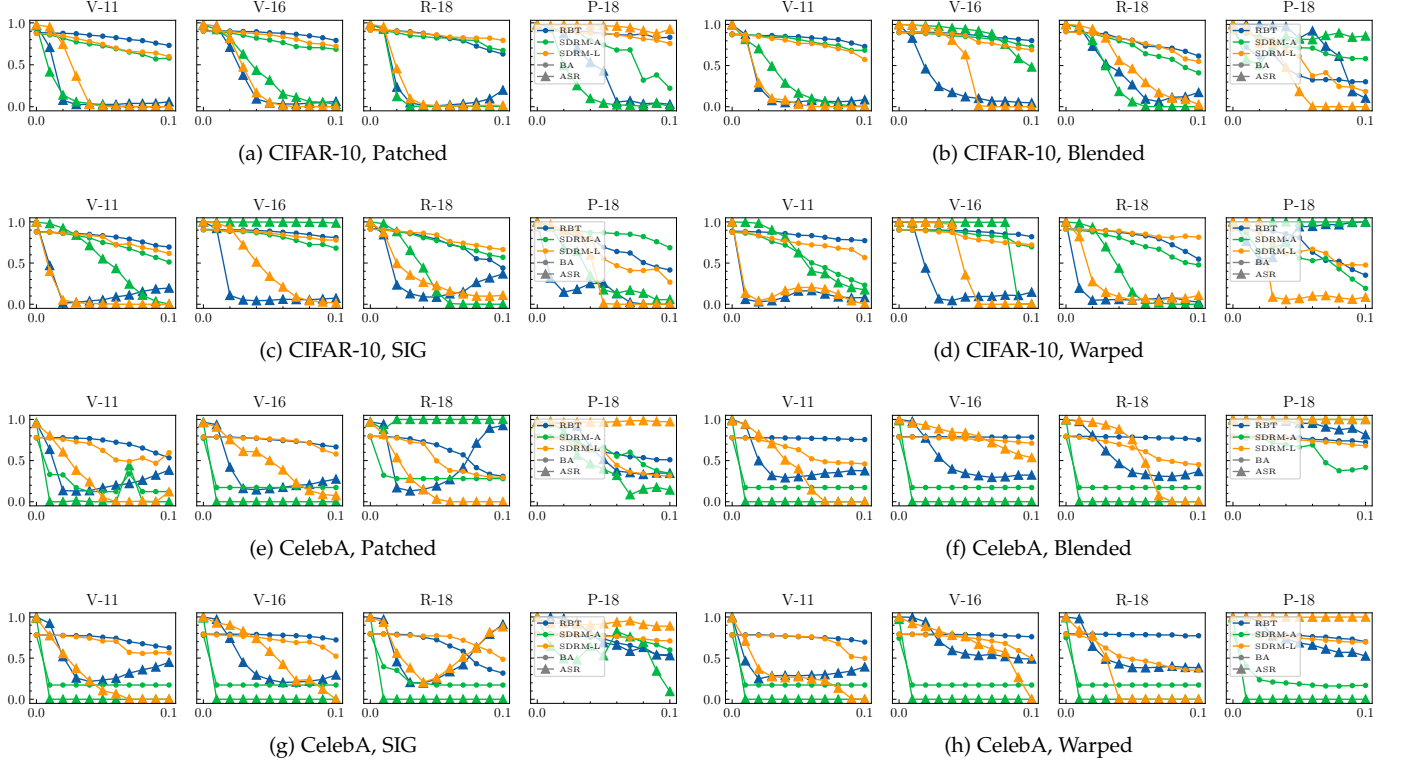


Fig. 10: BA and ASR of the infected models when pruning the trigger-related neurons. X-axis: the ratio of neurons pruned. Y-axis: the benign accuracy and the attack success rate.

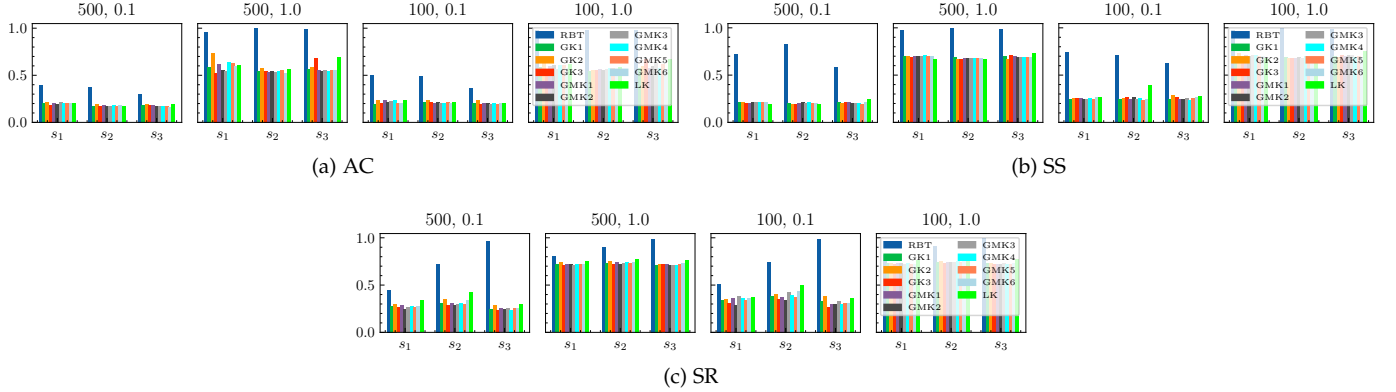


Fig. 11: F1 score of AC, SS, SR on the {CIFAR-10, P-18, Patched} models with different kernels.

et al. [46] proposed a training-free method by inserting a malicious module into the target model instead of perturbing the parameters.

The method we proposed in this paper can be used to enhance the above attacks to escape difference-based backdoor detection. As shown in Equation 4, SDRM adds a constraint item to the loss function without affecting the regular backdoor training.

8.2 Backdoor Defenses

Several defense approaches have been proposed to defend against these attacks, such as backdoor detection [?], [14], trigger synthesis [35], [48], model reconstruction [40], [49],

and model diagnosis [50], [51]. Among them, a vast number of defenses [14], [15], [21], [22], [52], [53], [54] distinguish backdoor samples from the clean ones by exploiting the statistical differences between clean and adversarial representations. Three typical methods have been introduced above, we here add some others. Chou et al. [53] leveraged the power of visualization tools, such as Grad-CAM [55], to inspect the backdoor behavior of poisoned models. Soremekun et al. [54] proposed a detection method similar to the activation clustering [14], which uses t-SNE as the dimensionality reduction and the mean-shift as the clustering algorithm. Hayase et al. [22] argued that the previous defense [15] works only when the spectral signature is large and proposed a method, SPECTRE, using robust covariance

estimation to amplify the signature of poisoned data.

However, our work demonstrates that the performance of difference-based detection methods can be greatly reduced when using infected models trained with SDRM. It calls for the need to study more powerful defense methods.

9 CONCLUSION

Our work studies the statistical differences between the features of clean and adversarial inputs in the infected model, which is the hypothesis of many detection methods. We identify that the statistical differences of multiple levels are all large enough to be used to distinguish inputs. Therefore, we propose a multi-level MMD reduction method and demonstrate that the differences can be significantly reduced without harming the attack intensity. Finally, the experimental results of three difference-based defenses, i.e., the activation clustering, the spectral signatures, and the subspace reconstruction, indicate that the defense effects decrease drastically as the differences reduce. The proposed method can enhance existing attacks to escape backdoor detection algorithms.

ACKNOWLEDGMENT

The work is partially supported by the National Natural Science Foundation of China under grand No.U19B2044 and No.61836011.

REFERENCES

- [1] R. Girshick, "Fast r-cnn," in *Proceedings of the IEEE international conference on computer vision*, 2015, pp. 1440–1448.
- [2] J. Long, E. Shelhamer, and T. Darrell, "Fully convolutional networks for semantic segmentation," in *Proceedings of the IEEE conference on computer vision and pattern recognition*, 2015, pp. 3431–3440.
- [3] J. Redmon and A. Farhadi, "Yolov3: An incremental improvement," *arXiv preprint arXiv:1804.02767*, 2018.
- [4] J. Yin, P. Xia, and J. He, "Online hard region mining for semantic segmentation," *Neural Processing Letters*, vol. 50, no. 3, pp. 2665–2679, 2019.
- [5] P. Xia, J. He, and J. Yin, "Boosting image caption generation with feature fusion module," *Multimedia Tools and Applications*, vol. 79, no. 33, pp. 24225–24239, 2020.
- [6] I. Sutskever, O. Vinyals, and Q. V. Le, "Sequence to sequence learning with neural networks," *arXiv preprint arXiv:1409.3215*, 2014.
- [7] Q. Chen, X. Zhu, Z. Ling, S. Wei, H. Jiang, and D. Inkpen, "Enhanced lstm for natural language inference," *arXiv preprint arXiv:1609.06038*, 2016.
- [8] J. Devlin, M.-W. Chang, K. Lee, and K. Toutanova, "Bert: Pre-training of deep bidirectional transformers for language understanding," *arXiv preprint arXiv:1810.04805*, 2018.
- [9] W. Chan, N. Jaitly, Q. Le, and O. Vinyals, "Listen, attend and spell: A neural network for large vocabulary conversational speech recognition," in *2016 IEEE International Conference on Acoustics, Speech and Signal Processing (ICASSP)*. IEEE, 2016, pp. 4960–4964.
- [10] D. Silver, A. Huang, C. J. Maddison, A. Guez, L. Sifre, G. Van Den Driessche, J. Schrittwieser, I. Antonoglou, V. Panneershelvam, M. Lanctot *et al.*, "Mastering the game of go with deep neural networks and tree search," *nature*, vol. 529, no. 7587, pp. 484–489, 2016.
- [11] R. Ying, R. He, K. Chen, P. Eksombatchai, W. L. Hamilton, and J. Leskovec, "Graph convolutional neural networks for web-scale recommender systems," in *Proceedings of the 24th ACM SIGKDD International Conference on Knowledge Discovery & Data Mining*, 2018, pp. 974–983.
- [12] J. Jumper, R. Evans, A. Pritzel, T. Green, M. Figurnov, O. Ronneberger, K. Tunyasuvunakool, R. Bates, A. Žídek, A. Potapenko *et al.*, "Highly accurate protein structure prediction with alpahofold," *Nature*, vol. 596, no. 7873, pp. 583–589, 2021.
- [13] T. B. Brown, B. Mann, N. Ryder, M. Subbiah, J. Kaplan, P. Dhariwal, A. Neelakantan, P. Shyam, G. Sastry, A. Askell *et al.*, "Language models are few-shot learners," *arXiv preprint arXiv:2005.14165*, 2020.
- [14] B. Chen, W. Carvalho, N. Baracaldo, H. Ludwig, B. Edwards, T. Lee, I. Molloy, and B. Srivastava, "Detecting backdoor attacks on deep neural networks by activation clustering," *arXiv preprint arXiv:1811.03728*, 2018.
- [15] B. Tran, J. Li, and A. Madry, "Spectral signatures in backdoor attacks," *arXiv preprint arXiv:1811.00636*, 2018.
- [16] X. Chen, C. Liu, B. Li, K. Lu, and D. Song, "Targeted backdoor attacks on deep learning systems using data poisoning," *arXiv preprint arXiv:1712.05526*, 2017.
- [17] T. Gu, B. Dolan-Gavitt, and S. Garg, "Badnets: Identifying vulnerabilities in the machine learning model supply chain," *arXiv preprint arXiv:1708.06733*, 2017.
- [18] Y. Liu, S. Ma, Y. Aafer, W.-C. Lee, J. Zhai, W. Wang, and X. Zhang, "Trojaning attack on neural networks," 2017.
- [19] M. Xue, C. He, J. Wang, and W. Liu, "One-to-n & n-to-one: Two advanced backdoor attacks against deep learning models," *IEEE Transactions on Dependable and Secure Computing*, 2020.
- [20] E. Wenger, J. Passananti, A. N. Bhagoji, Y. Yao, H. Zheng, and B. Y. Zhao, "Backdoor attacks against deep learning systems in the physical world," in *Proceedings of the IEEE/CVF Conference on Computer Vision and Pattern Recognition*, 2021, pp. 6206–6215.
- [21] K. Jin, T. Zhang, C. Shen, Y. Chen, M. Fan, C. Lin, and T. Liu, "A unified framework for analyzing and detecting malicious examples of dnn models," *arXiv preprint arXiv:2006.14871*, 2020.
- [22] J. Hayase, W. Kong, R. Somani, and S. Oh, "Spectre: Defending against backdoor attacks using robust statistics," *arXiv preprint arXiv:2104.11315*, 2021.
- [23] T. J. L. Tan and R. Shokri, "Bypassing backdoor detection algorithms in deep learning," *arXiv preprint arXiv:1905.13409*, 2019.
- [24] M. Barni, K. Kallas, and B. Tondi, "A new backdoor attack in cnns by training set corruption without label poisoning," in *2019 IEEE International Conference on Image Processing (ICIP)*. IEEE, 2019, pp. 101–105.
- [25] A. Nguyen and A. Tran, "Wanet-imperceptible warping-based backdoor attack," *arXiv preprint arXiv:2102.10369*, 2021.
- [26] A. Gretton, K. M. Borgwardt, M. J. Rasch, B. Schölkopf, and A. Smola, "A kernel two-sample test," *The Journal of Machine Learning Research*, vol. 13, no. 1, pp. 723–773, 2012.
- [27] A. Krizhevsky, G. Hinton *et al.*, "Learning multiple layers of features from tiny images," 2009.
- [28] Z. Liu, P. Luo, X. Wang, and X. Tang, "Deep learning face attributes in the wild," in *Proceedings of the IEEE international conference on computer vision*, 2015, pp. 3730–3738.
- [29] A. Turner, D. Tsipras, and A. Madry, "Label-consistent backdoor attacks," *arXiv preprint arXiv:1912.02771*, 2019.
- [30] A. Salem, R. Wen, M. Backes, S. Ma, and Y. Zhang, "Dynamic backdoor attacks against machine learning models," *arXiv preprint arXiv:2003.03675*, 2020.
- [31] K. Simonyan and A. Zisserman, "Very deep convolutional networks for large-scale image recognition," *arXiv preprint arXiv:1409.1556*, 2014.
- [32] K. He, X. Zhang, S. Ren, and J. Sun, "Deep residual learning for image recognition," in *Proceedings of the IEEE conference on computer vision and pattern recognition*, 2016, pp. 770–778.
- [33] ———, "Identity mappings in deep residual networks," in *European conference on computer vision*. Springer, 2016, pp. 630–645.
- [34] M. Javaheripi, M. Samragh, G. Fields, T. Javidi, and F. Koushanfar, "Cleann: Accelerated trojan shield for embedded neural networks," in *2020 IEEE/ACM International Conference On Computer Aided Design (ICCAD)*. IEEE, 2020, pp. 1–9.
- [35] B. Wang, Y. Yao, S. Shan, H. Li, B. Viswanath, H. Zheng, and B. Y. Zhao, "Neural cleanse: Identifying and mitigating backdoor attacks in neural networks," in *2019 IEEE Symposium on Security and Privacy (SP)*. IEEE, 2019, pp. 707–723.
- [36] Y. Li, B. Wu, Y. Jiang, Z. Li, and S.-T. Xia, "Backdoor learning: A survey," *arXiv preprint arXiv:2007.08745*, 2020.
- [37] A. Paszke, S. Gross, S. Chintala, G. Chanan, E. Yang, Z. DeVito, Z. Lin, A. Desmaison, L. Antiga, and A. Lerer, "Automatic differentiation in pytorch," 2017.

- [38] C. Liao, H. Zhong, A. Squicciarini, S. Zhu, and D. Miller, "Backdoor embedding in convolutional neural network models via invisible perturbation," *arXiv preprint arXiv:1808.10307*, 2018.
- [39] S. Li, M. Xue, B. Zhao, H. Zhu, and X. Zhang, "Invisible backdoor attacks on deep neural networks via steganography and regularization," *IEEE Transactions on Dependable and Secure Computing*, 2020.
- [40] Y. Liu, Y. Xie, and A. Srivastava, "Neural trojans," in *2017 IEEE International Conference on Computer Design (ICCD)*. IEEE, 2017, pp. 45–48.
- [41] Y. Liu, X. Ma, J. Bailey, and F. Lu, "Reflection backdoor: A natural backdoor attack on deep neural networks," in *European Conference on Computer Vision*. Springer, 2020, pp. 182–199.
- [42] Y. Li, T. Zhai, B. Wu, Y. Jiang, Z. Li, and S. Xia, "Rethinking the trigger of backdoor attack," *arXiv preprint arXiv:2004.04692*, 2020.
- [43] J. Dumford and W. Scheirer, "Backdooring convolutional neural networks via targeted weight perturbations," in *2020 IEEE International Joint Conference on Biometrics (IJCB)*. IEEE, 2018, pp. 1–9.
- [44] K. Kurita, P. Michel, and G. Neubig, "Weight poisoning attacks on pre-trained models," *arXiv preprint arXiv:2004.06660*, 2020.
- [45] A. S. Rakin, Z. He, and D. Fan, "Tbt: Targeted neural network attack with bit trojan," in *Proceedings of the IEEE/CVF Conference on Computer Vision and Pattern Recognition*, 2020, pp. 13 198–13 207.
- [46] R. Tang, M. Du, N. Liu, F. Yang, and X. Hu, "An embarrassingly simple approach for trojan attack in deep neural networks," in *Proceedings of the 26th ACM SIGKDD International Conference on Knowledge Discovery & Data Mining*, 2020, pp. 218–228.
- [47] S. Wang, S. Nepal, C. Rudolph, M. Grobler, S. Chen, and T. Chen, "Backdoor attacks against transfer learning with pre-trained deep learning models," *IEEE Transactions on Services Computing*, 2020.
- [48] H. Chen, C. Fu, J. Zhao, and F. Koushanfar, "Deepinspect: A black-box trojan detection and mitigation framework for deep neural networks," in *IJCAI*, 2019, pp. 4658–4664.
- [49] Y. Li, X. Lyu, N. Koren, L. Lyu, B. Li, and X. Ma, "Neural attention distillation: Erasing backdoor triggers from deep neural networks," *arXiv preprint arXiv:2101.05930*, 2021.
- [50] X. Xu, Q. Wang, H. Li, N. Borisov, C. A. Gunter, and B. Li, "Detecting ai trojans using meta neural analysis," *arXiv preprint arXiv:1910.03137*, 2019.
- [51] S. Kolouri, A. Saha, H. Pirsavash, and H. Hoffmann, "Universal litmus patterns: Revealing backdoor attacks in cnns," in *Proceedings of the IEEE/CVF Conference on Computer Vision and Pattern Recognition*, 2020, pp. 301–310.
- [52] K. Liu, B. Dolan-Gavitt, and S. Garg, "Fine-pruning: Defending against backdooring attacks on deep neural networks," in *International Symposium on Research in Attacks, Intrusions, and Defenses*. Springer, 2018, pp. 273–294.
- [53] E. Chou, F. Tramèr, and G. Pellegrino, "Sentinet: Detecting localized universal attacks against deep learning systems," in *2020 IEEE Security and Privacy Workshops (SPW)*. IEEE, 2020, pp. 48–54.
- [54] E. Soremekun, S. Udeshi, S. Chattopadhyay, and A. Zeller, "Exposing backdoors in robust machine learning models," *arXiv preprint arXiv:2003.00865*, 2020.
- [55] R. R. Selvaraju, M. Cogswell, A. Das, R. Vedantam, D. Parikh, and D. Batra, "Grad-cam: Visual explanations from deep networks via gradient-based localization," in *Proceedings of the IEEE international conference on computer vision*, 2017, pp. 618–626.

APPENDIX

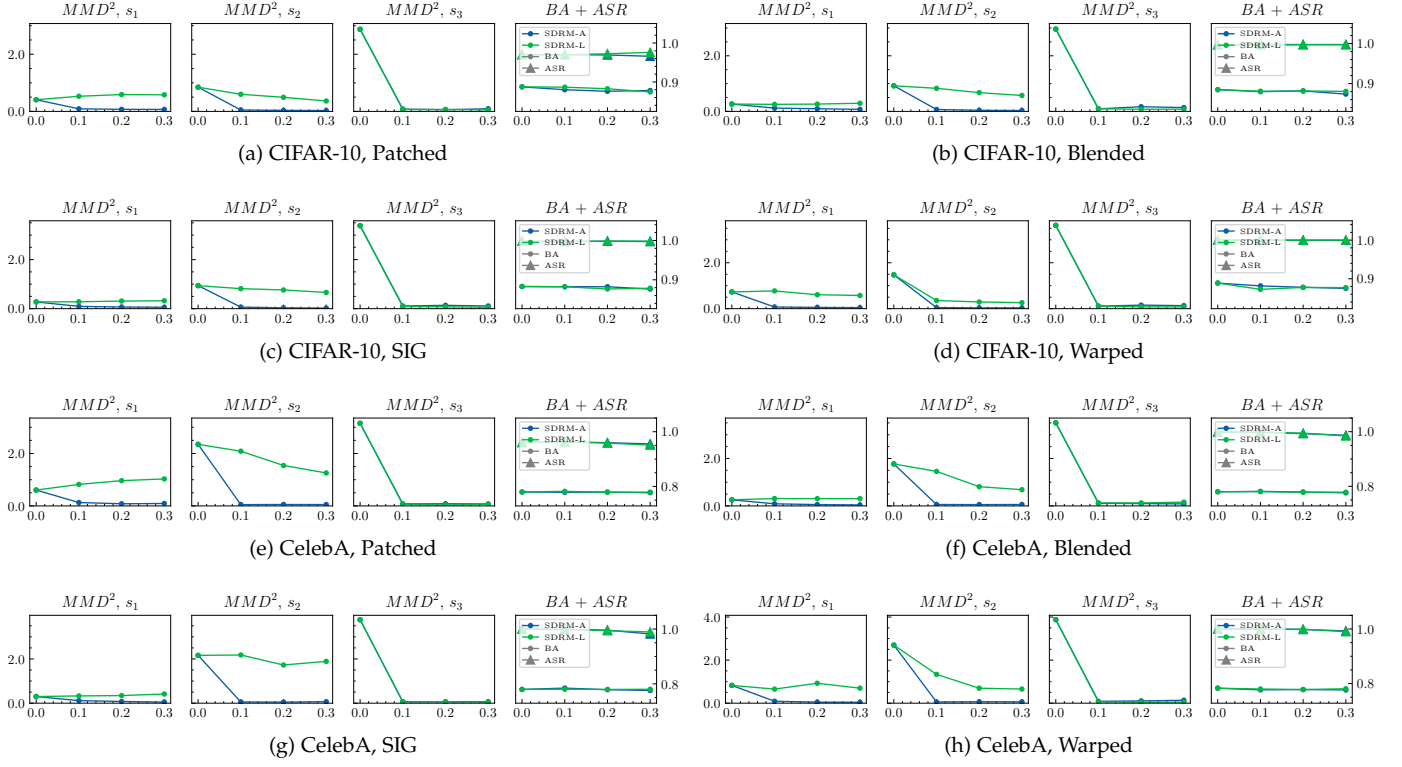


Fig. 12: Results of SDRM on the {V-11} models with different λ . X-axis: the value of λ . Y-axis: the value of each indicator.

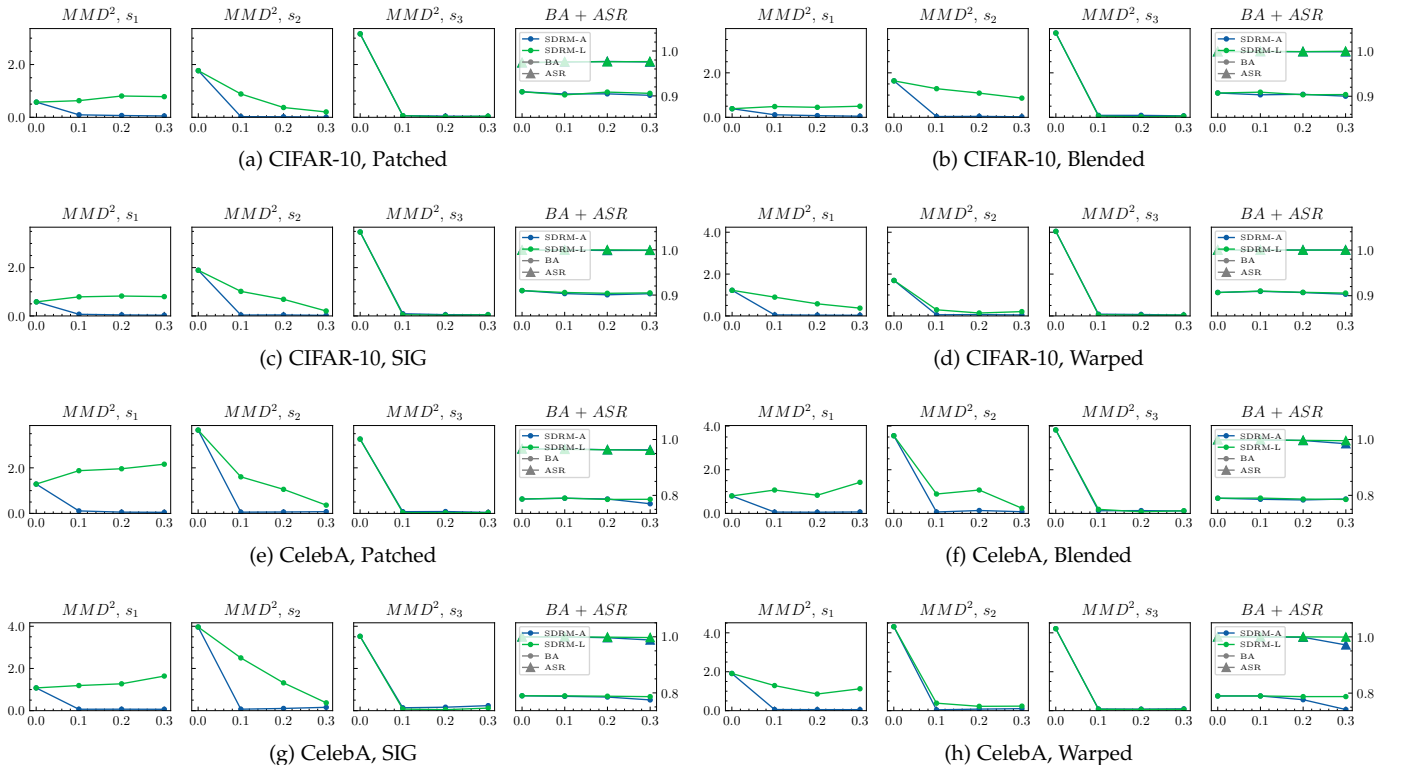


Fig. 13: Results of SDRM on the {V-16} models with different λ . X-axis: the value of λ . Y-axis: the value of each indicator.

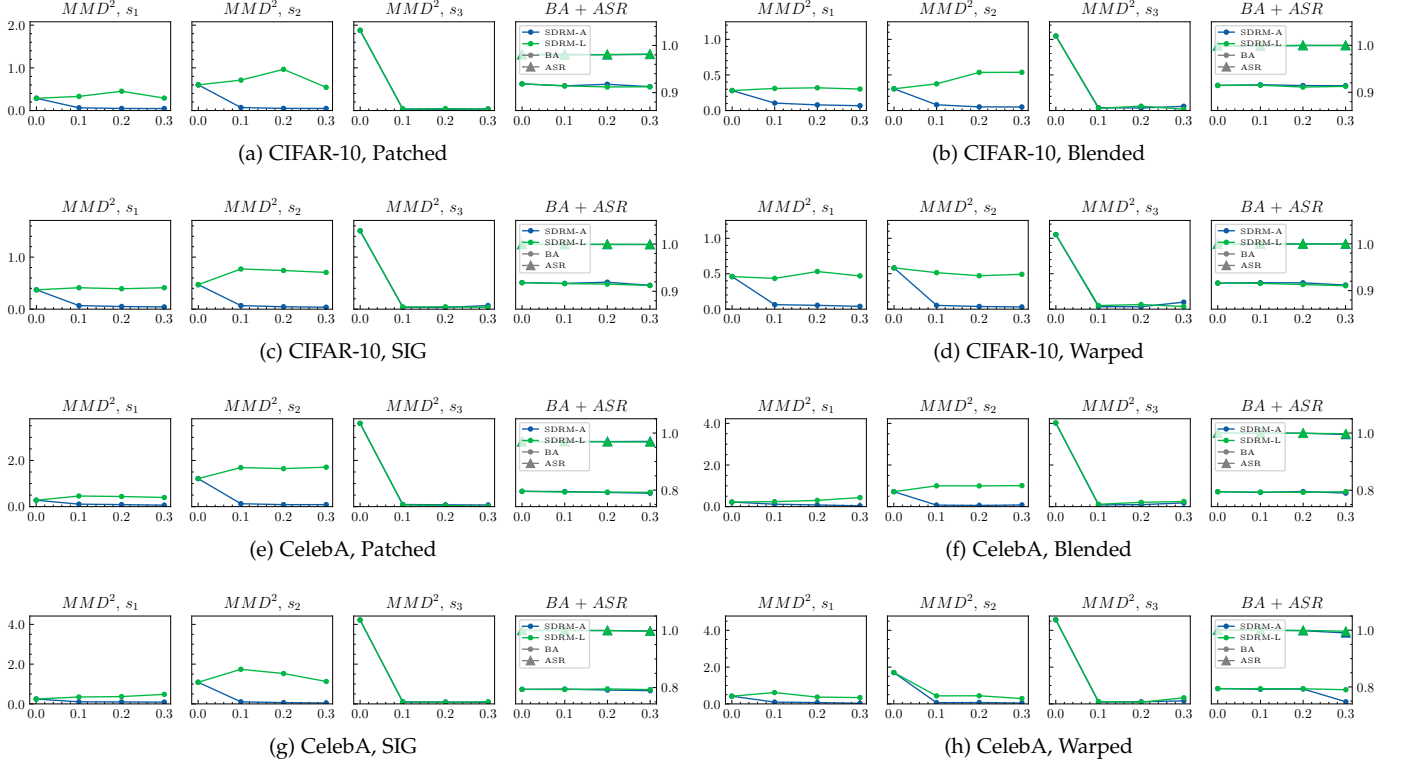


Fig. 14: Results of SDRM on the {R-18} models with different λ . X-axis: the value of λ . Y-axis: the value of each indicator.

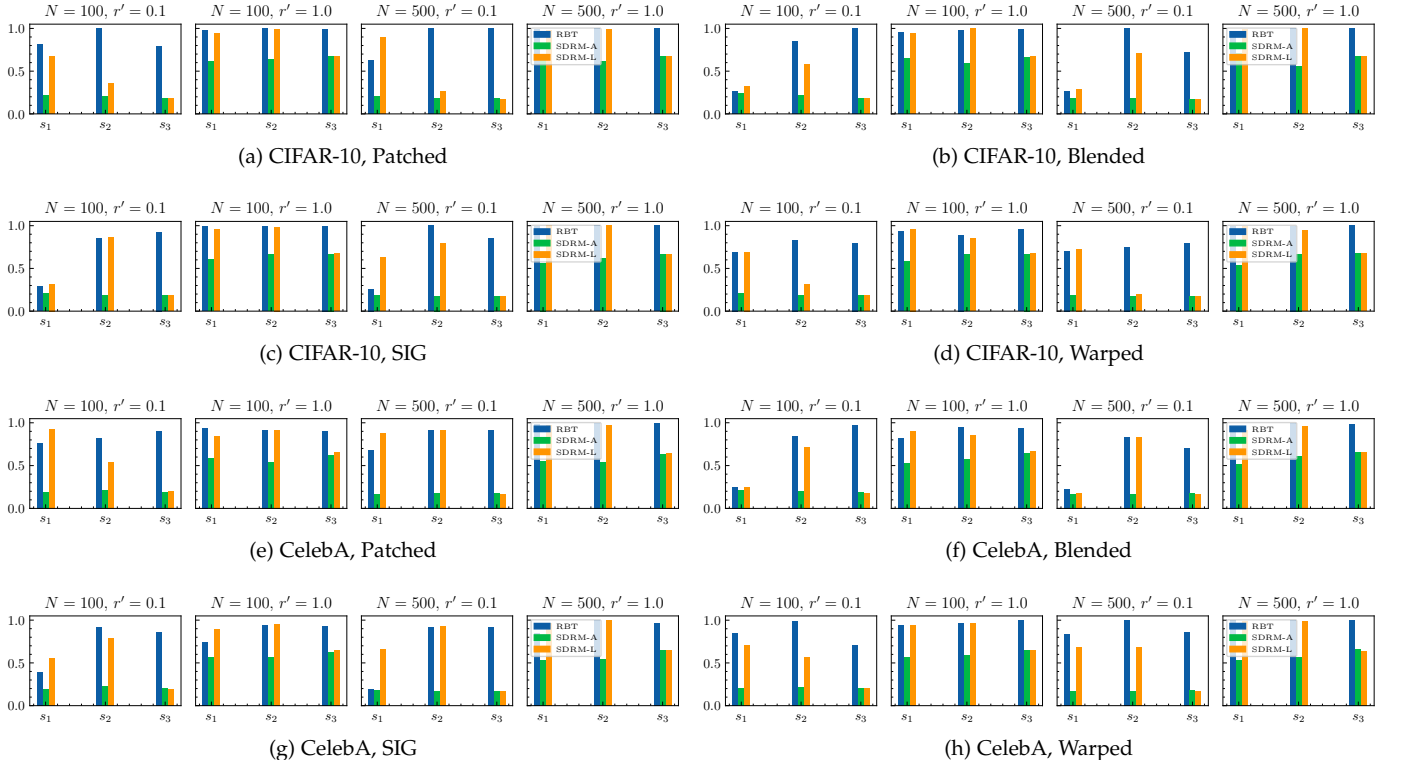


Fig. 15: F1 score of AC on the {V-11} models. X-axis: the level of features. Y-axis: the value of $F1$.

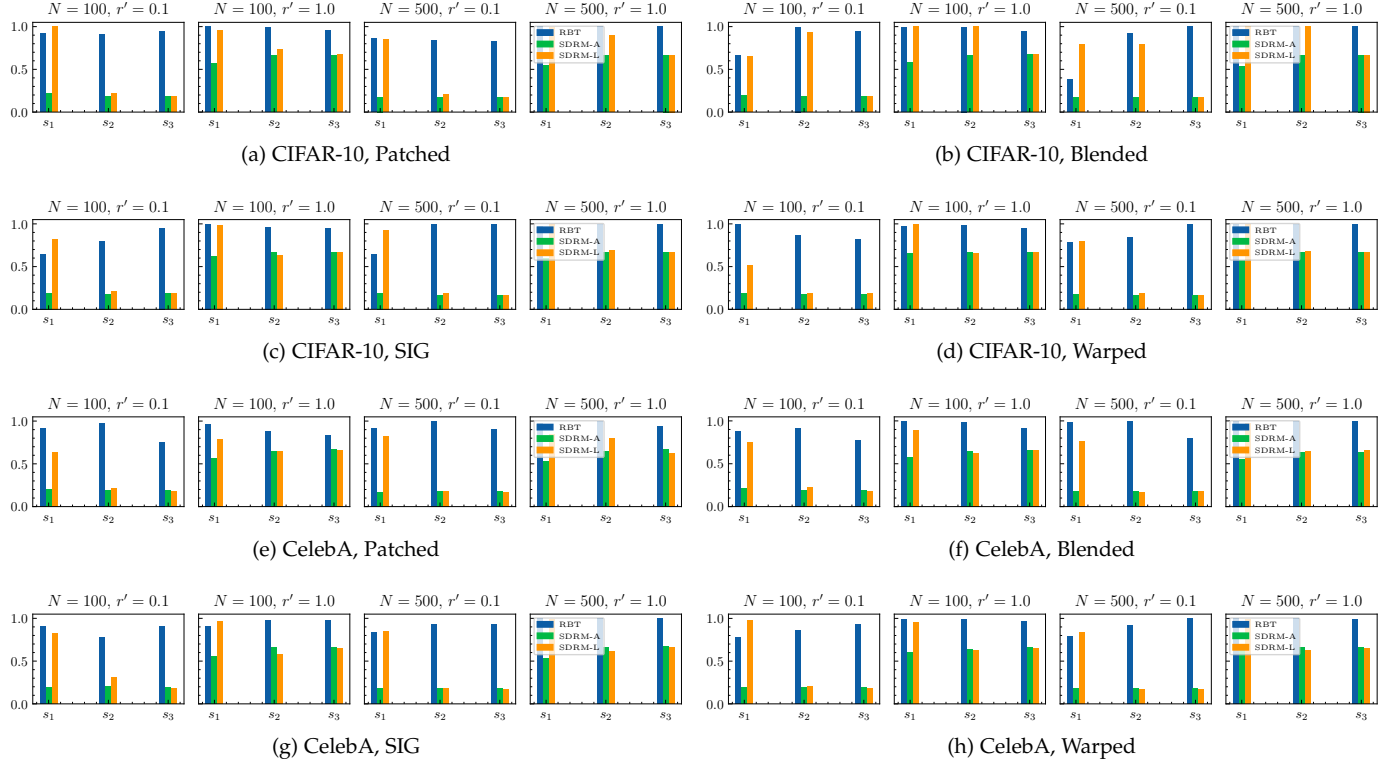


Fig. 16: F1 score of AC on the $\{V-16\}$ models. X-axis: the level of features. Y-axis: the value of $F1$.

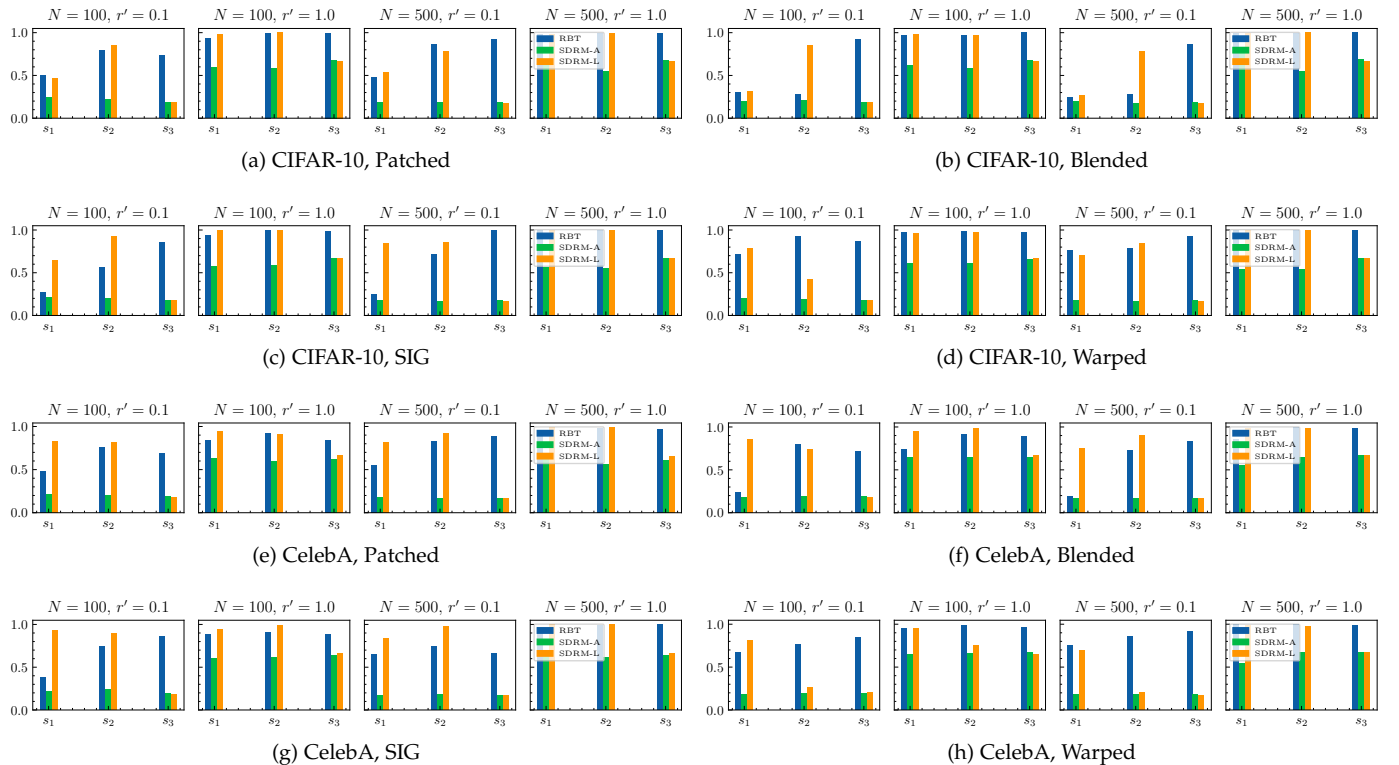


Fig. 17: F1 score of AC on the $\{R-18\}$ models. X-axis: the level of features. Y-axis: the value of $F1$.

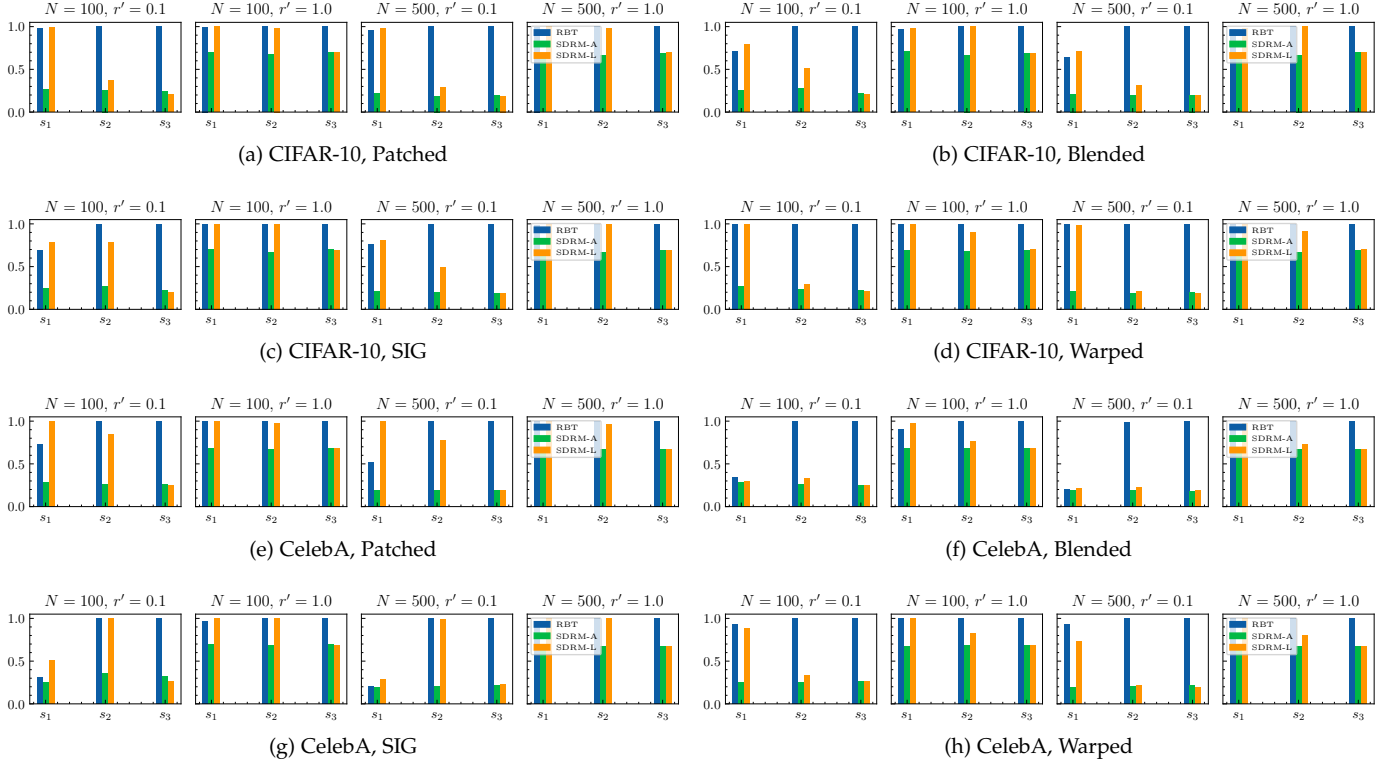


Fig. 18: F1 score of SS on the {V-11} models. X-axis: the level of features. Y-axis: the value of $F1$.

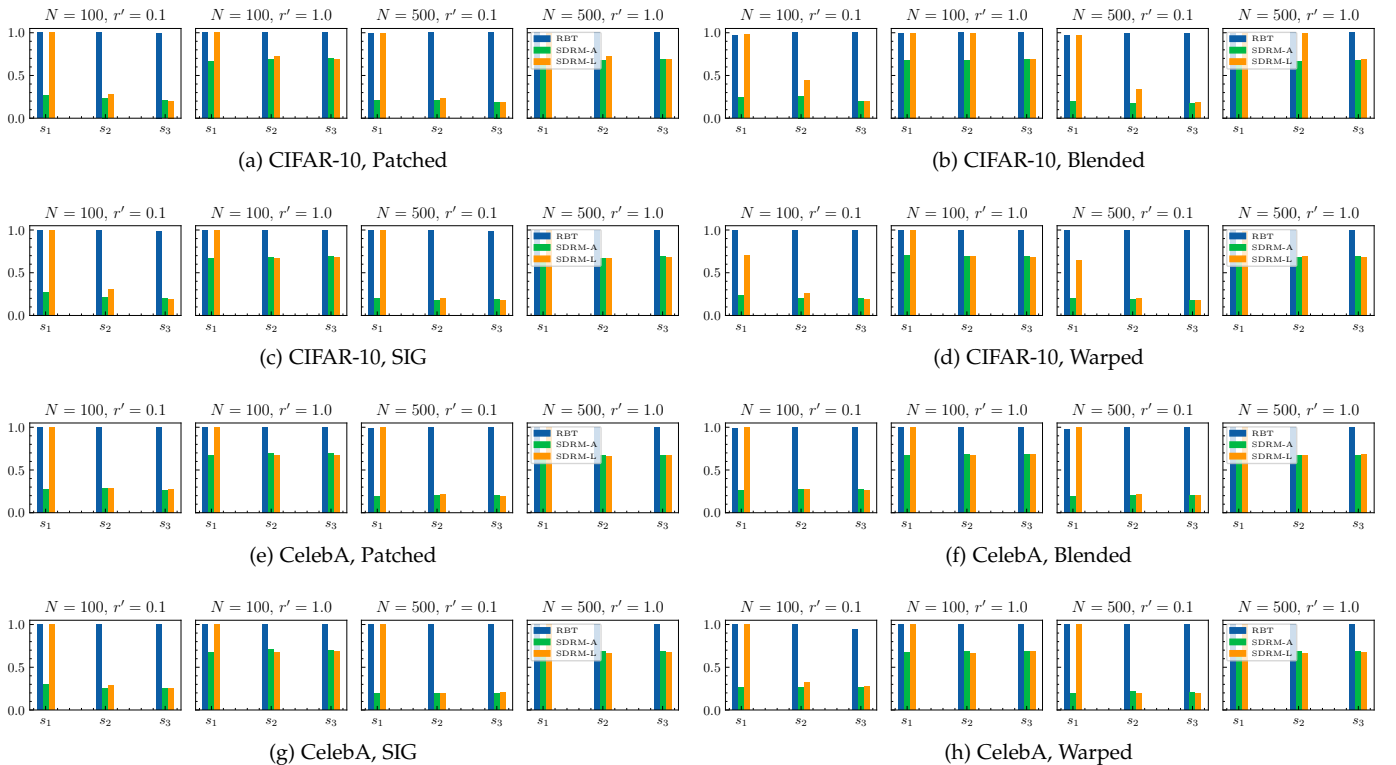


Fig. 19: F1 score of SS on the {V-16} models. X-axis: the level of features. Y-axis: the value of $F1$.

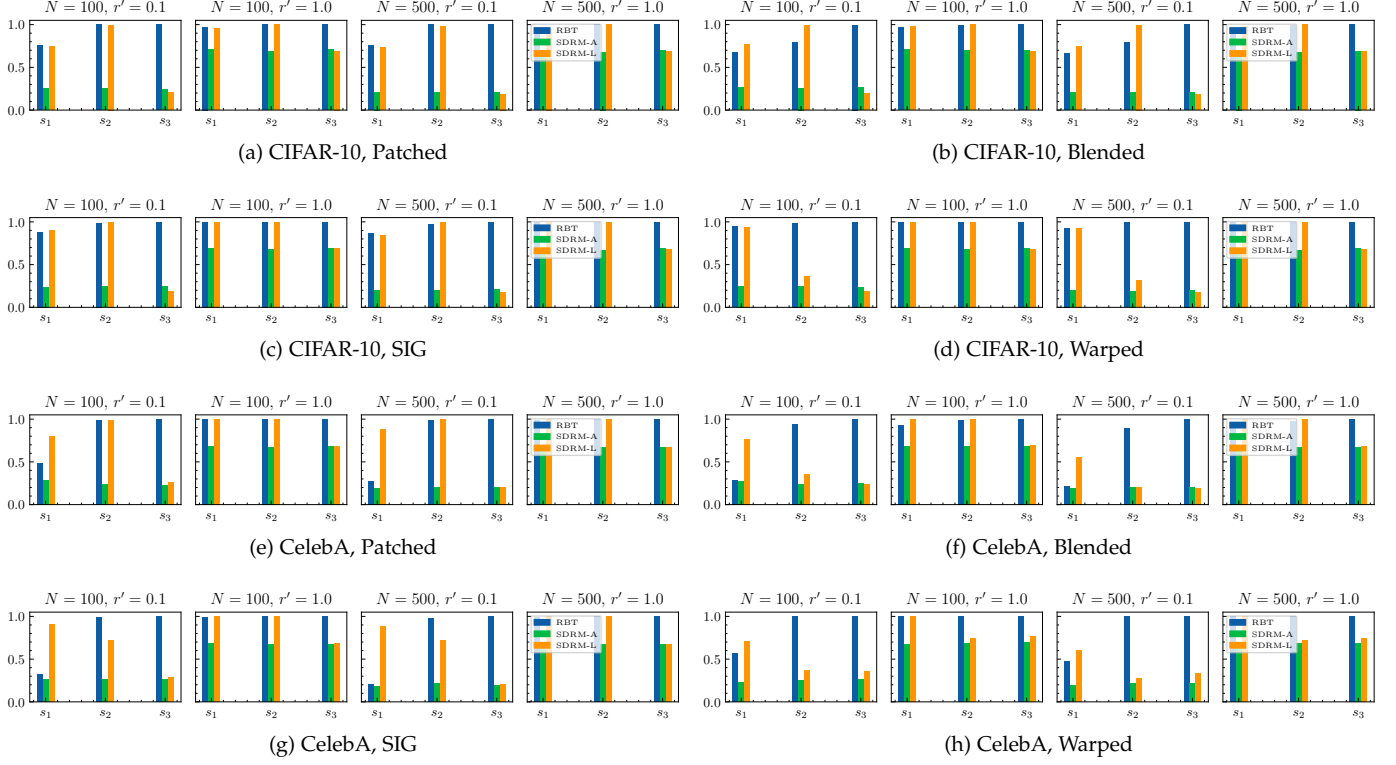


Fig. 20: F1 score of SS on the $\{R-18\}$ models. X-axis: the level of features. Y-axis: the value of $F1$.

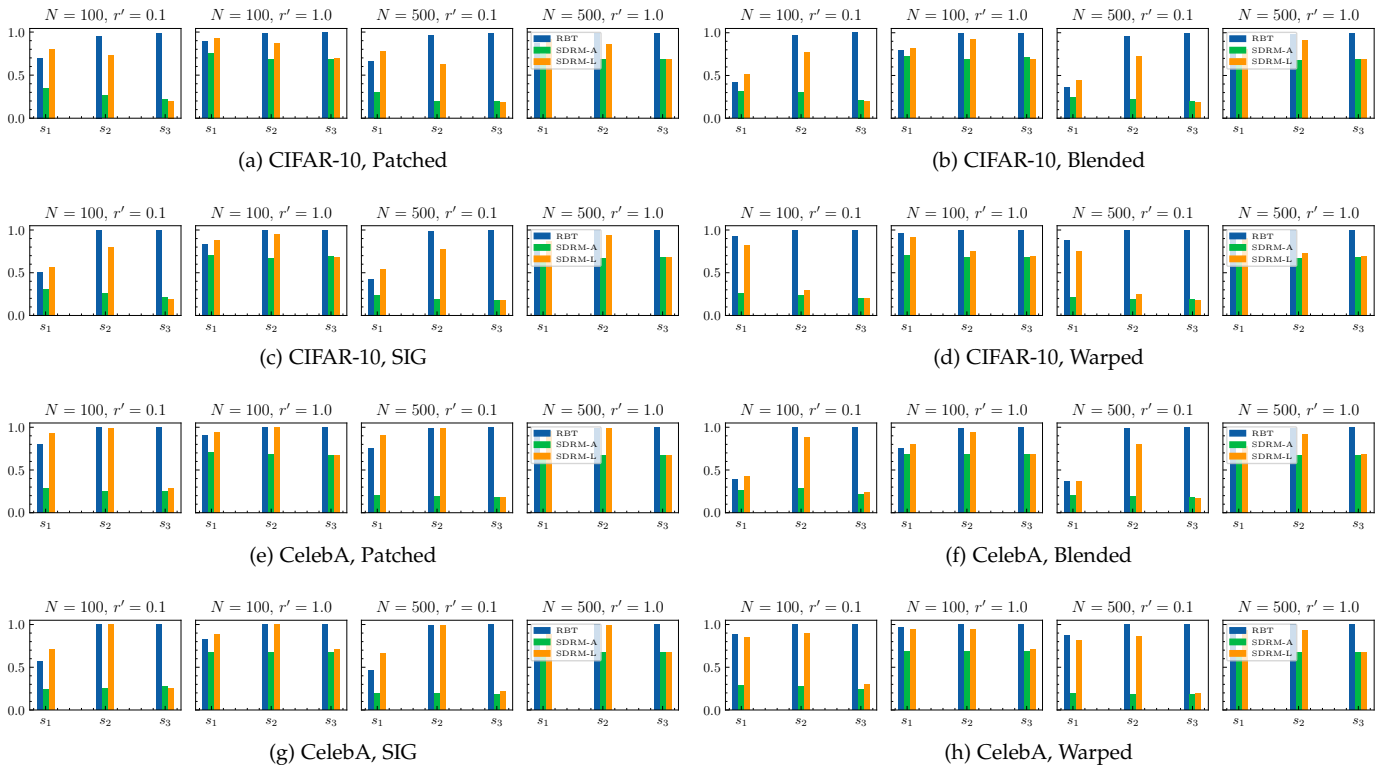


Fig. 21: F1 score of SR on the $\{V-11\}$ models. X-axis: the level of features. Y-axis: the value of $F1$.

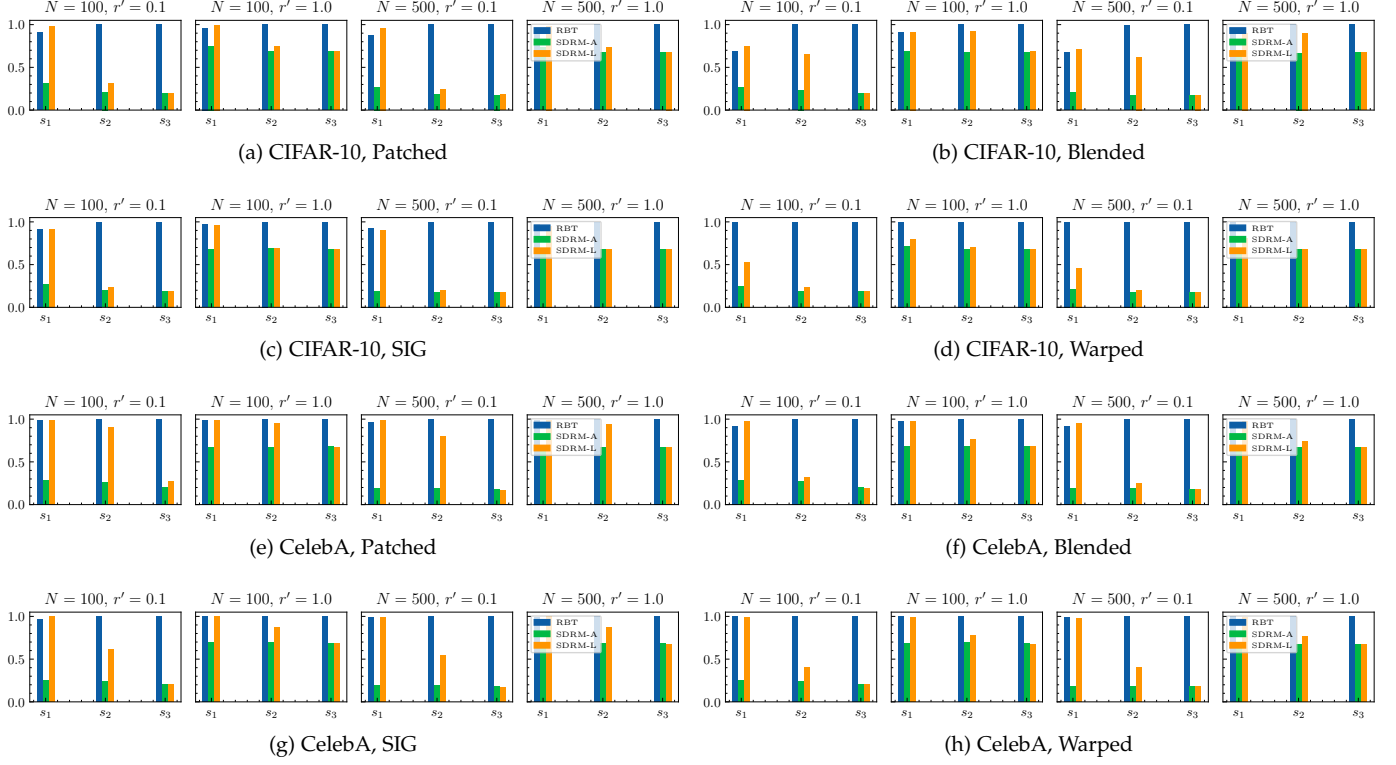


Fig. 22: F1 score of SR on the $\{V-16\}$ models. X-axis: the level of features. Y-axis: the value of $F1$.

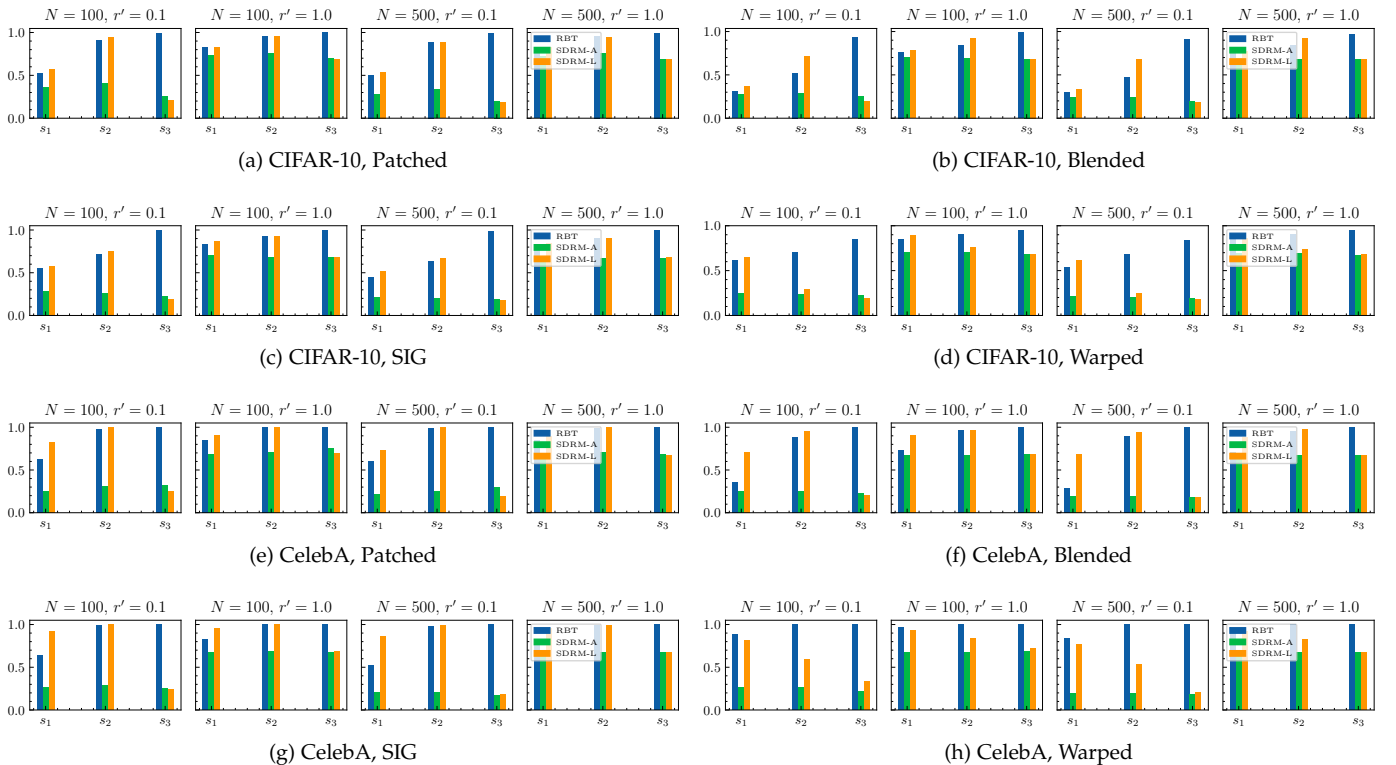


Fig. 23: F1 score of SR on the $\{R-18\}$ models. X-axis: the level of features. Y-axis: the value of $F1$.